

UNIVERSITÉ DU QUÉBEC À CHICOUTIMI

MÉMOIRE PRÉSENTÉ À  
L'UNIVERSITÉ DU QUÉBEC À CHICOUTIMI COMME  
EXIGENCE PARTIELLE  
DE LA MAÎTRISE EN INGÉNIERIE

Par

JALIL FARZANEH-DEHKORDI

**EXPERIMENTAL STUDY AND MATHEMATICAL  
MODELING OF FLASHOVER OF EHV  
INSULATORS COVERED WITH ICE**

JULY 2004



### Mise en garde/Advice

Afin de rendre accessible au plus grand nombre le résultat des travaux de recherche menés par ses étudiants gradués et dans l'esprit des règles qui régissent le dépôt et la diffusion des mémoires et thèses produits dans cette Institution, **l'Université du Québec à Chicoutimi (UQAC)** est fière de rendre accessible une version complète et gratuite de cette œuvre.

Motivated by a desire to make the results of its graduate students' research accessible to all, and in accordance with the rules governing the acceptance and diffusion of dissertations and theses in this Institution, the **Université du Québec à Chicoutimi (UQAC)** is proud to make a complete version of this work available at no cost to the reader.

L'auteur conserve néanmoins la propriété du droit d'auteur qui protège ce mémoire ou cette thèse. Ni le mémoire ou la thèse ni des extraits substantiels de ceux-ci ne peuvent être imprimés ou autrement reproduits sans son autorisation.

The author retains ownership of the copyright of this dissertation or thesis. Neither the dissertation or thesis, nor substantial extracts from it, may be printed or otherwise reproduced without the author's permission.

## Abstract

One of the major problems in cold climate regions is ice accretion on power network equipment, including cables, conductors, and insulators. In addition to mechanical problems caused by the combined effects of ice and wind, ice on insulators is at the origin of a loss in electrical insulating strength, sometimes resulting in flashover faults and consequent power outages. A number of studies have been carried out in several laboratories over the past 30 years and particularly at UQAC over the past 25 years. These studies deal with many aspects of atmospheric icing, including the field observation of ice accretion, laboratory experiments on the electrical performance of insulators under ice or snow conditions, as well as fundamental studies on flashover of ice-covered insulators. Among the many realizations at UQAC, a mathematical model has been developed for predicting the flashover voltage of ice-covered insulators. However, due to the complex laboratory conditions required, this model has not been validated for engineering application to long ice-covered EHV insulators.

The overall objective of this Master's thesis is to study the flashover phenomenon on full-scale, ice-covered EHV insulators, in order to improve the existing mathematical model for predicting the minimum flashover voltage such insulators. This study contributes to the understanding of the flashover phenomenon on ice-covered EHV insulators and presents a powerful tool for the design of outdoor insulators in cold climate regions.

Three units of standard shape post insulators, similar to those typically used in Hydro-Quebec 735 kV substations, were submitted to laboratory investigation on the electrical performance of EHV insulators under icing conditions. A series of tests were carried out for 2 different applied water conductivities and 5 dry arcing distances, to determine the relationship between the minimum flashover voltage of ice-covered insulators and the insulator length, up to full scale. It was found that  $V_{WS}$  increases in a slightly non-linear manner with an increase in insulator dry-arcing distance. Further,  $V_{MF}$  of a 2 m insulator arcing distance was 195 kV<sub>rms</sub> for the melting regime and 190 kV<sub>rms</sub> icing regime, for an applied water conductivity of 30  $\mu$ S/cm and an ice thickness of 15 mm, as measured on a rotating monitoring cylinder. These voltages are about 7 % and 9 % lower than the service voltage of the insulators, respectively. Based on these results and using multi-arcing model, an improved mathematical model

was proposed for predicting the minimum flashover voltage of EHV insulators under icing conditions. There is good concordance between experimental results and those calculated from the improved model.

Finally, based on the study presented in this thesis, several recommendations for further research interests are proposed.

## Résumé

L'accumulation de glace sur les équipements des réseaux électriques, incluant câbles, conducteurs et isolateurs, représente l'un des problèmes majeurs rencontrés dans les régions au climat froid. En plus des problèmes mécaniques causés par les effets combinés de la glace et du vent, la glace sur les isolateurs est à l'origine d'une perte de facteur d'isolation, ce qui occasionne parfois des contournements et conséquemment, des pannes d'électricité. Bon nombre d'études en laboratoire se sont penchées sur cette problématique depuis une trentaine d'années, et particulièrement à l'UQAC depuis 25 ans. Ces études se concentrent sur plusieurs aspects du givrage atmosphérique, incluant l'observation de l'accumulation de glace dans des sites naturels, des expériences en laboratoire sur la performance électrique des isolateurs dans des conditions de glace et de neige, ainsi que des études fondamentales du contournement des isolateurs recouverts de glace. Parmi les progrès réalisés à l'UQAC, un modèle mathématique a été développé afin de prédire la tension de contournement des isolateurs recouverts de glace. Toutefois, en raison de la complexité des infrastructures requises, le modèle n'a pu être validé pour des applications d'ingénierie sur de longs isolateurs extra-haute-tension recouverts de glace.

L'objectif principal de cette recherche, dans le cadre d'études de 2<sup>e</sup> cycle, est celui d'étudier le phénomène du contournement sur des isolateurs extra-haute-tension recouverts de glace, afin d'améliorer le modèle mathématique existant, qui permettra de prédire la tension de contournement minimale de tels isolateurs. Cette étude contribuera à une meilleure compréhension du phénomène du contournement des isolateurs extra-haute-tension recouverts de glace et le modèle sera un outil indispensable pour la conception d'isolateurs pour usage extérieur dans les régions froides. Trois unités d'isolateurs de poste de forme standard, tels que ceux utilisés dans les poste à 735 kV d'Hydro-Québec, ont été soumis à des tests en laboratoire afin d'en déterminer la performance électrique dans des conditions de givrage. Une série de tests a été effectuée à 2 niveaux différents de conductivité d'eau d'accumulation et 5 distances d'arc, afin de déterminer la relation entre la tension de contournement minimale des isolateurs recouverts de glace et la longueur des isolateurs,

jusqu'à pleine échelle. Il a été déterminé que la  $V_{WS}$  (tension de tenue maximale) augmente de façon légèrement non linéaire avec l'augmentation de la longueur d'arc. Aussi, la  $V_{MF}$  (tension de contournement minimale) pour une distance d'arc de 2 m s'établit à  $195 \text{ kV}_{rms}$  en régime de fonte et à  $190 \text{ kV}_{rms}$  en régime de givrage, pour une conductivité d'eau d'accumulation de  $30 \mu\text{S/cm}$  et une épaisseur de glace de  $15 \text{ mm}$ , telle que mesurée sur un cylindre témoin en rotation. Ces niveaux de tension sont approximativement 7 % et 9 % plus bas que la tension de service des isolateurs, respectivement. D'après ces résultats et en utilisant un modèle à arcs multiples, un modèle mathématique amélioré a été proposé pour la prédiction de la tension de contournement minimale des isolateurs extra-haute-tension dans des conditions de givrage. Il y a bonne concordance entre les résultats des expériences en laboratoire et ceux de modèle amélioré.

Finalement, en se basant sur l'étude présentée dans ce mémoire, plusieurs recommandations peuvent être faites en vue de recherches connexes à venir.

## Acknowledgments

This Master's research was carried out within the framework of the Industrial Chair on Atmospheric Icing of power Network Equipment (CIGELE) at the University of Quebec in Chicoutimi (UQAC).

I would like to use this window of opportunity to thank those who helped me complete this thesis. First, I would like to express my sincere appreciation to my Director, Professor Masoud Farzaneh, for his supervision, guidance, support, and patience, as well as his generous help during my Masters' studies. I would also like to express my gratitude to my co-director, Dr. Jianhui Zhang, for his guidance and help during my project. Thank you as well to Mr. Talbot for his linguistic support.

I would like to show my deepest appreciations to all of my friends and collaborators who helped and encouraged me during in my work, and especially to my parents, to who have always stood behind me and to whom I am debtor for everything.

Finally, I have kept my warmest thanks to my spouse Mandana Javan, whose patience and encouraging words were essential to the completion of this project.

# Contents

<b>ABSTRACT.....</b>	<b>II</b>
<b>RÉSUMÉ.....</b>	<b>IV</b>
<b>ACKNOWLEDGEMENTS.....</b>	<b>VI</b>
<b>CONTENTS.....</b>	<b>VII</b>
<b>LIST OF FIGURES.....</b>	<b>XI</b>
<b>LIST OF TABLES.....</b>	<b>XIII</b>
<b>LIST OF ABBREVIATIONS AND SYMBOLS.....</b>	<b>XIV</b>
<b>LIST OF PAPERS PUBLISHED FROM THIS THESIS.....</b>	<b>XVII</b>
<b>CHAPTER 1 INTRODUCTION.....</b>	<b>1</b>
1.1. General.....	2
1.2. Problem Definition.....	2
1.3. Research Objectives.....	5
1.4. Methodology.....	6
1.5. Statement of Originality.....	7
1.6. Organization of Thesis.....	8
<b>CHAPTER 2 REVIEW OF LITERATURE.....</b>	<b>10</b>
2.1. Introduction.....	11
2.2. Discharge in air gaps.....	12
2.2.1. Primary Avalanche initiation.....	12
2.2.2. Secondary Avalanches and First Corona.....	14

2.2.3. Dark Period.....	15
2.2.4. Leader.....	15
2.2.5. Final Jump.....	17
2.3. Flashover on Polluted Surfaces.....	17
2.3.1. General Description.....	17
2.3.2. Modeling of Arc on Polluted Insulators.....	21
2.3.2.1. DC Models.....	21
2.3.2.2. AC Models.....	23
2.4. Flashover of ice-covered insulators.....	25
2.4.1. Description of Flashover on ice-covered Surfaces.....	25
2.4.2. Factors Influencing $V_{MF}$ of Ice-Covered Insulators.....	27
2.4.2.1. Influence of Insulator Type and Configuration.....	28
2.4.2.2. Influence of Insulator Lengths.....	29
2.4.2.3. Influence of Ice Type and Density.....	30
2.4.2.4. Influence of Amount of Ice.....	32
2.4.2.5. Influence of Applied Water Conductivity.....	33
2.4.3. Modeling of Flashover on Ice-covered Insulators.....	35
2.5. Conclusion.....	43
<b>Chapter 3 Experimental Facilities and Test Procedures.....</b>	<b>45</b>
3.1. Introduction.....	46
3.2. Facilities used in this study.....	46
3.2.1. Test Insulators .....	46
3.2.2. Climate Room.....	47

3 . 2 . 3 . Water Droplet Generator.....	50
3 . 2 . 4 . Cooling System.....	52
3 . 2 . 5 . High Voltage System.....	52
3 . 2 . 6 . Data Acquisition System.....	53
3 . 2 . 7 . Test Circuit.....	55
3.3. Test Procedures.....	56
3 . 3 . 1 . Ice Thickness Measurement.....	56
3 . 3 . 2 . Evaluating the Flashover Voltage of Ice-Covered Insulators.....	58
3 . 3 . 2 . 1 . Melting Regime Method.....	58
3 . 3 . 2 . 2 . Icing Regime Method.....	63
<b>Chapter 4 Experimental results and discussions.....</b>	<b>65</b>
4.1. Introduction.....	66
4.2. Observation of flashover on EHV ice-covered insulators.....	66
4.3. Comparison of evaluating methods.....	69
4.4. Experimental results.....	71
4.5. Conclusions.....	75
<b>Chapter 5 Modeling of Flashover on Ice-Covered EHV Insulators.....</b>	<b>76</b>
5.1. Introduction.....	77
5.2. Improvement of the existing model.....	80
5.3. Validation of the improved model.....	84
5.4. Application of the model.....	87
5 . 4 . 1 . Effect of insulator diameter on $V_{MF}$ .....	87
5 . 4 . 2 . Effect of conductivity on $V_{MF}$ .....	88

5.4.3. Critical arc length and critical leakage current.....	88
<b>Chapter 6 Conclusions and Recommendations.....</b>	<b>92</b>
6.1. Conclusions .....	93
6.2. Recommendations.....	95
<b>References.....</b>	<b>97</b>

## List of Figures

Figure 2-1. Critical volume in a positive discharge sequence.....	13
Figure 2-2. Streamer-leader schematic representation.....	16
Figure 2-3. Flashover process on polluted surface.....	20
Figure 2-4. Obenaus model of flashover on a polluted surface.....	21
Figure 2-5. Arc inception and development on an ice-covered insulator.....	27
Figure 2-6. Maximum withstand stress as a function of the ice thickness.....	33
Figure 2-7. Variation of $V_{WS}$ of insulators as a function of applied water conductivity.....	34
Figure 2-8. Model for flashover on ice-covered insulators.....	36
Figure 2-9. Ice sample used for determining arc parameters.....	38
Figure 2-10. Typical waveforms of static model.....	40
Figure 2-11. E-I curve of arc on ice surface.....	41
Figure 2-12. Application of the model to 5 IEEE standard insulators.....	43
Figure 3-1. Standard porcelain station post insulator.....	48
Figure 3-2. Dry-arcing distance of ice-covered insulators.....	49
Figure 3-3. Interior of the climate room.....	50
Figure 3-4. Pneumatic nozzle.....	52
Figure 3-5. HV transformer with its associated regulator.....	53
Figure 3-6. Data acquisition system.....	54
Figure 3-7. LABVIEW interface designed for data gathering.....	54
Figure 3-8. Test circuit.....	55

Figure 3-9. Rotating and fixed monitoring cylinders.....	57
Figure 3-10. Ice on monitoring conductors.....	57
Figure 3-11. Monitoring conductors installed at different positions.....	58
Figure 3-12. Sequences of “melting regime” test procedure.....	59
Figure 3-13. Sequences of “icing regime” test procedure.....	64
Figure 4-1. Accumulation of ice layer on insulator surface.....	67
Figure 4-2. Two arcs along the air gaps.....	68
Figure 4-3. Propagation of arcs on ice surface.....	69
Figure 4-4. Compare of two melting regime and icing regime.....	70
Figure 4-5. $V_{MF}$ as a function of dry arcing distance ( $\sigma = 30 \mu\text{S/cm}$ ).....	72
Figure 4-6. $V_{MF}$ as a function of dry arcing distance ( $\sigma = 80 \mu\text{S/cm}$ )... ..	74
Figure 5-1. Comparison between the experimental and calculated results ( $\sigma = 80\mu\text{S/cm}$ ).....	79
Figure 5-2. Comparison between the experimental and calculated results ( $\sigma = 30\mu\text{S/cm}$ ).....	79
Figure 5-3. Two arcs on insulator.....	80
Figure 5-4. Double arcs model.....	81
Figure 5-5. Equivalent model.....	81
Figure 5-6. The interface of improved model.....	84
Figure 5-7. Experimental results and those calculated from the improved model ( $\sigma = 80 \mu \text{ S/cm}$ ).....	85
Figure 5-8. Experimental results and those calculated from the improved model ( $\sigma = 30 \mu \text{ S/cm}$ ).....	86
Figure 5-9. $V_{MF}$ as a function of insulator diameter.....	87
Figure 5-10. Effect of freezing water on VMF.....	88
Figure 5-11. Critical arc length as a function of dry arcing distance.....	90

## List of Tables

Table 2-1 Characteristics of ice formed on structures.....	30
Table 2-2 Experimental conditions for dry-grown and wet-grown ice.....	31
Table 3-1 Test parameters for the ice accretion sequence.....	61
Table 4-1 Test results for different dry arcing distances ( $\sigma = 30 \mu\text{S/cm}$ ).....	72
Table 4-2 Test tests for different insulator lengths ( $\sigma = 80 \mu\text{S/cm}$ ).....	73
Table 5-1 Comparison between the experimental and calculated results ( $\sigma = 80\mu\text{S/cm}$ ).....	78
Table 5-2 Comparison between the experimental and calculated results ( $\sigma = 30\mu\text{S/cm}$ ).....	78
Table 5-3 Comparison of experimental results and those from the improved model for the STD porcelain post insulators ( $\sigma = 80 \mu \text{ S/cm}$ ).....	85
Table 5-4 Comparison of experimental results and those from the improved model for the STD porcelain post insulator ( $\sigma = 30 \mu \text{ S/cm}$ ).....	86
Table 5-5 Critical current calculated from the improved model.....	91

## LIST OF ABBREVIATIONS AND SYMBOLS

A	Arc constant
$b^*$	Exponent of AC arc recovery condition
b	Exponent of AC arc re-ignition conditions
EHV	Extra High Voltage
EPDM	Ethylene Propylene Diene Monomers
CIGELE	Industrial Chair on Atmospheric Icing of Power Network Equipment (in French acronym CIGELE)
CIGRE	International Council on Large Electric Systems
DAS	Data acquisition system
DC+	Positive direct voltage
DC-	Negative direct voltage
d	Ice Thickness
D	Insulator diameter
$E_{arc}$	Voltage gradient along arc
$E_{MF}$	Minimum Flashover gradient
I	Leakage current
$I_c$	Critical leakage current
$I_m$	Peak value of ac current
$k^*$	AC arc recovery constant

$k$	AC arc re-ignition constant
$L$	Total Insulator length
$n$	Exponent of arc characteristic
$P$	Power taken from the supply
$R(x)$ or $R_p$	Resistance of the part of the ice which is not bridged by arc.
$r$	Arc foot radius
$r_p$	Uniform pollution resistance per unit leakage path
SiR	Silicone Rubber
STD	Standard
$T$	Temperature
$V_e$	Voltage drop on electrodes
$U_c$	Critical voltage
$U_{cx}$	Critical voltage as a function of $x$
UQAC	Université du Québec a Chicoutimi
$V_a$	Applied voltage at arc extinction time
$V_b$	Applied voltage at breakdown
$V$	Applied voltage
$V_c$	Critical flashover voltage
$V_{cx}$	Minimum DC voltage to sustain the arc bridging a portion of $x/L$ of the leakage path $L$
$V_m$	Peak values of AC voltage
$V_{MF}$	Minimum Flashover Voltage

$V_{ws}$	Maximum Withstand Voltage
$x$	Length of arc
$x_c$	Critical arc length
$\sigma$	Freezing water conductivity
$\gamma_e$	Equivalent surface conductivity of the ice sample during flashover
$W$	Width of the polluted strip.

## **List of Papers Published Based on the Results of this M.S. Thesis**

1. J. Farzaneh-Dehkordi, J. Zhang and M. Farzaneh, “Experimental Study and Modeling of Flashover Performance of EHV Insulators Covered with Ice”. 61<sup>st</sup> Eastern Snow Conference, Portland, Maine, USA, June 2004 (Selected as the best Paper of student Competition and winner of Wiesnet Medal).
2. M. Farzaneh, J-F. Drapeau, J. Zhang, M.J. Roy & J. Farzaneh-Dehkordi, “Flashover performance of transmission class insulators under icing conditions”. Insulator News and Market Report Conference, Marbella, Spain, pp. 315-326, August 2003.
3. M. Farzaneh, J. Farzaneh-Dehkordi, and J. Zhang, “Flashover Performance of EHV Station Post Insulators Covered with Ice”, CEIDP conference Colorado, USA, October 2004.
4. M. Farzaneh, J. Zhang, and J. Farzaneh-Dehkordi, “Modeling of Flashover on Ice-Covered EHV Insulators”, 7th IASTED International Conference on Power and energy systems ,Clearwater Beach , USA, Nov 2004.

**CHAPTER 1**  
**INTRODUCTION**

# **Chapter 1**

## **Introduction**

### **1.1 General**

With industrial development, electric power supply is becoming more and more important in modern societies. Due to the continuous increase of the need for electricity, long distance power transmission lines and high voltage substations have been widely used in power networks. The safe operation of power systems depends on many factors, one of which being the insulating components, in particular various types of insulators, which play an increasingly important role. Most insulators are used outdoors, on high voltage overhead transmission lines and in substations, and are required to withstand extreme changes in environmental conditions.

### **1.2 Problem definition**

In cold climate regions, one of the major problems for power systems is atmospheric icing. The ice accumulated on power transmission lines and devices, due to freezing rain or drizzle, in-cloud icing, icing fog, wet snow, or frost may lead to mechanical damages

and/or electrical faults, sometimes resulting in power failures and the consequent troubles to community services and daily life. Power outages caused by ice and snow accretion have been reported by many authors in various countries such as Canada [37], the United States [4], Japan [30] [46], Norway [26], China [55], and England [29].

Major parts of Canada are located in cold climate regions. The most serious power failure in Canadian history occurred in January 1998, when an uncommon ice storm hit parts of southern and western Quebec, eastern Ontario and part of the Atlantic Provinces. Over the period of January 5-9, about 100 mm of freezing rain fell on these regions. Ice accretion resulted in the collapse of more than 1,000 towers (including 735 kV power transmission lines), and 30,000 wooden poles. Close to 1.4 million people in Quebec and 230,000 in Ontario were without power for several days. One month after the ice storm, 700,000 people were still without electricity. The direct economic loss for a single power company, Hydro-Quebec, was approximately one billion Canadian dollars [37].

In addition to the mechanical damages, the ice accreted on insulators can decrease their insulating strength considerably and may, on occasion, result in flashover faults. Some power outages related to this phenomenon have also been reported in several countries [25] [54] subjected to northern climatic conditions. In Canada, a typical example occurred March 9-10, 1986, within the Ontario Hydro network. Due to freezing rain and fog, the surface of the insulators accumulated ice and short icicles, which resulted in 57 successive flashovers, resulting in the breakdown of the most part of the 500 kV transmission systems in southern Ontario [31] . Again, other flashover incidents took place on April 18, 1988, at

the Arnaud substation in the Hydro-Quebec network. A series of six flashovers, caused by insulators covered with wet snow, resulted in a major power interruption for a large part of the province [38].

Flashover phenomena on ice-covered insulators have attracted a great deal of attention from many researchers and a large number of studies have been carried out in several laboratories on the subject [5] [6] [14] [26] [30] [33] [56] [55] [57]. Normally, experimental or in-the-field investigation is costly and time-consuming. Therefore, many attempts have been made individually or by research groups to establish mathematical models for predicting the flashover voltage of ice-covered insulators [19] [21] [23]. As a result, such a model was developed at CIGELE and has been successfully applied to insulators of up to 1 m in length [23]. However, despite these efforts, many aspects of the flashover phenomena on ice-covered insulators, particularly on EHV insulators, are still not well understood. Also, because of the limiting conditions of laboratories, experimental results for the flashover voltage of full scale EHV insulators under icing conditions are scarce. This situation makes it difficult to apply this model to long ice-covered insulators for engineering purposes. Therefore, further studies are needed to further advance knowledge on this phenomenon and the mathematical model needs to be improved for application to long insulators under icing conditions.

### 1.3 Research objectives

The overall objectives of this thesis are to study flashover on long insulators and to improve the existing mathematical model for predicting the critical flashover voltage of full-scale EHV insulators. The specific objectives are:

- Observation of the flashover process on ice-covered EHV post insulators, with a dry-arcing distance of up to 4.17 m, corresponding to that of full-scale insulators used in 735 kV substations.
- Comparison of two experimental methods developed at CIGELE for evaluating the flashover performance of ice-covered insulators. One suitable method will be chosen to determine the minimum flashover voltage of ice-covered insulators in this study.
- Investigation of the flashover performance of full-scale EHV insulators under icing conditions. The relation between the minimum flashover voltage of ice-covered insulators and the insulator dry-arcing distance will be determined.
- Improvement of the mathematical model. The existing model will be compared to the experimental results, and the necessary improvements will be made for

application to EHV insulators, based on experimental results and those of previous studies.

## 1.4 Methodology

In order to achieve the objectives of this study, a series of laboratory experiments were carried out in one of the CIGELE climate rooms. The results were subjected to both theoretical and mathematical analyses. The main methods used in this study may be summarized as follows:

- Using the facilities at CIGELE, an ice layer, with a thickness of 15 mm measured on the rotating monitoring cylinder, was formed on standard porcelain post-type insulators.
- Using a set of AC high voltage sources and a data acquisition system, the minimum flashover voltage of the insulators was determined under icing conditions, by means of an “icing regime” method, for 5 dry-arcing distances varying from 1.39 m to 4.17 m, and 2 different applied water conductivities.
- Using regression analysis, the relationship between the minimum flashover voltage of ice-covered insulators and the dry-arcing distance was determined.

- Based on the experimental results, the existing mathematical model was improved by modifying the arc re-ignition constants and taking into consideration the multi-arc effect.
- A program was written in MATLAB for predicting the flashover voltage of ice-covered EHV insulators. A user interface was created for easy calculation and engineering applications.

## **1.5 Statement of originality**

By means of the test facilities at CIGELE and the test methods developed in previous studies, the flashover performance of EHV post insulators, typically used in Hydro-Quebec 735 kV power substations, was investigated under icing conditions. The observation and analysis to the test process and results contributed to the advancement of knowledge of the flashover phenomena on long insulators covered with ice.

Based on the results, the mathematical model for predicting the flashover voltage of ice-covered EHV insulators was improved. This model is a powerful tool for the design of outdoor insulators for use in cold climate regions.

## 1.6 Organization of the Thesis

This thesis is divided into six chapters, beginning with a basic statement and literature available on the subject, and makes it possible for the reader to follow the test principles and modeling process, as well as their results.

The present chapter is an overall introduction for this Masters' thesis. In this chapter, the problem, research objectives, methods used, and main contributions of this study are briefly described.

In the second chapter, some related fundamental theories on the electrical breakdown in air gaps and flashover on polluted or ice-covered surfaces are presented, particularly for flashover of ice-covered insulators, including the ice accretion process and affecting parameters, arc propagation, and flashover mechanisms. Then, a review of literature follows, which summarizes the results of previous studies related to the subject of this thesis from two aspects: experimental results and mathematical model for flashover on ice-covered insulators. These reviews will help the reader understand the choice of experimental parameters and the improvement of the existing model in this study.

In relation with the objectives introduced and parameters selected, the facilities were chosen and are presented in Chapter 3. The facilities used in the study, such as (i) cooling system, (ii) wind generating system, (iii) water spray system; (iv) high voltage system, and (v) measuring system are explained. Then, the two methods for evaluating the flashover

performance of ice-covered insulators, that is the “icing regime” and “melting regime” methods are detailed.

The experimental results are presented in Chapter 4. First, the effects of the test methods on the evaluating results are investigated. Selecting a suitable method, the flashover performance of EHV standard porcelain post insulators was tested and the relationship between the minimum flashover voltage and the insulator dry-arcing distance was determined. At the end of this chapter, the results are discussed.

Chapter 5 focuses on the modeling of the flashover of ice-covered insulators. Based on the experimental results, the reasons behind the error in application of the existing mathematical model to long insulators are first analyzed and the necessary improvements are proposed. A MATLAB program and the corresponding user interface are also presented in this chapter. The calculated results are validated by the experimental results and a good concordance between them is obtained.

Finally, in Chapter 6, some general conclusions are summarized from analyses and discussions of the results reported in the previous chapters. In addition, some recommendations are provided for future research.

**CHAPTER 2**

**REVIEW OF LITERATURE**

## Chapter 2

### Review of Literature

#### 2.1 Introduction

Atmospheric ice accretion on power transmission lines has been studied by researchers worldwide for many years [5] [6] [14] [26] [30] [33] [55] [61]. It has also been studied for over 25 years at the Research Group on Atmospheric Environment Engineering (GRIEA) and the later-created NSERC/Hydro-Quebec/UQAC Chair on Atmospheric Icing of Power Network Equipment (CIGELE) in the University of Quebec in Chicoutimi (UQAC) [51]. A large number of creditable publications have been released and several review papers have been completed by Farzaneh *et al* [13] [23].

In order to better understand the mechanisms underlying flashover on ice-covered insulators, as well as the background of this study, a review of the literature on related topics is presented in this chapter, including the physics of discharge, and corona initiation and development in air gaps.

Flashover on ice-covered insulators is similar to that on polluted insulators and ice may be considered a special type of pollution [23]. A mathematical model similar to that used

for flashover on polluted insulators has been developed for ice-covered insulators [19] [23] [27]. Therefore, a brief review on the flashover and arc modeling on polluted insulators is also made in this chapter.

Finally, some fundamental studies on the mechanisms underlying the flashover on ice-covered insulators, the parameters affecting the performance of ice-covered insulators, and the mathematical modeling of arc on iced surfaces are reviewed.

## **2.2 Discharge in air gaps**

The flashover on ice surfaces is a kind of surface discharge along the interface of air and ice surface. It is actually a breakdown of air, particularly during the formation of local arcs along air gaps. Therefore, the theory of electrical discharges in air is helpful for understanding this phenomenon. This process can be described as follow [28]:

### **2.2.1 Primary avalanche initiation**

Ice accretion along an insulator is not uniform because of ice shedding or discharge activities. Normally, parts of insulator remain ice-free, and, hereafter, these zones will be called air gaps. The heating effect of leakage current or sunshine leads to the creation of a water film on the ice surface, which has a relatively high conductivity. This highly conductive water film will result in that most of the applied voltage will drop along air gaps

and produce a relatively high electric field in these zones. When the electric field is strong enough, corona inception occurs.

In fact, a few electrons are always present in the air gaps, by means of UV radiation from the sun, for one. If at least one electron falls within the critical volume (Fig. 2.1), where the electric field strength ( $E$ ) is higher than the critical strength of air ( $E_c$ ), electron avalanches, which are called “primary avalanches”, will be created by electron collision.

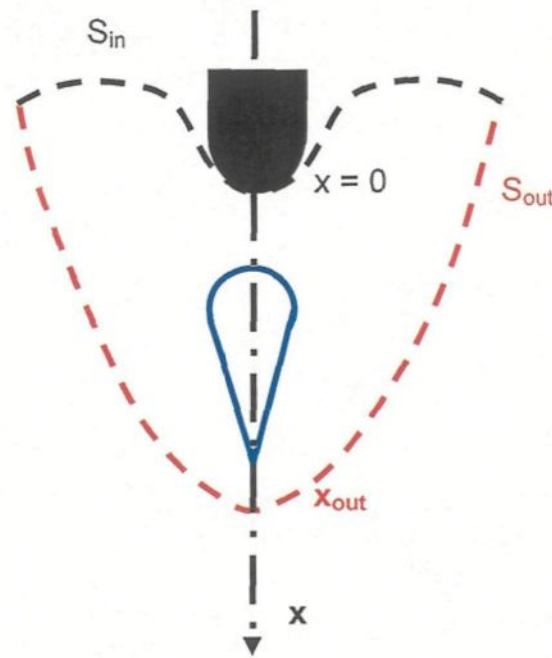


**Fig.2.1 Critical volume in a positive discharge sequence [28]**

This critical volume is defined by two conditions [28]:

- The electric field must be strong enough ( $E \geq E_c$ ) and the electrons must be placed in the region where  $\alpha - \eta > 0$  ( $\alpha$  and  $\eta$  represent the ionization and attachment coefficients of the gas, respectively)
- The avalanche triggered by the germ electron must develop over a sufficient distance in order to generate a streamer

In the critical volume, electrons will be accelerated by the electric field. They will ionize neutral particles by collision. Newly created electrons are subjected to the same field and also ionize other neutral particles, and so on. Then, an electron avalanche, which is developed from the movement of the germ electrons towards the anode, is produced. The quasi-stationary positive ions will remain behind it. The mobility of the electrons is approximately one hundred to one thousand times higher than that of ions. The high density created space charge will distort the applied electric field.

### **2.2.2 Secondary avalanches and first corona**

The head of the primary avalanche is the origin of the emission of photons, due to combination or attachment of charged particles. The primary avalanche reaches the anode and the photons are absorbed by surrounding gas. Depending on the energy of photons, they may produce other electrons. If the electron produced is located in the vicinity of the primary avalanches, it will create a new avalanche, called “secondary avalanche”, according to the same mechanisms as previously mentioned.

The secondary avalanche will travel directly towards the tail of the primary avalanche. The presence of residual positive ions brings some local changes to the electric field and gives rise to a “hair” of luminous filaments of conical form escaping from electrodes that called “streamer”. It is the first visible luminous demonstration close to the high voltage electrode.

### **2.2.3 Dark Period**

In attend of a divergent electric field, the first corona effect can be followed by one or more periods, between which other corona effects are intercalated. Because no ionizing activity can take place during this period, it is called “dark period”, in which the field is reduced below  $E_c$  by the space charge injected by the first corona. Indeed, the latter tends to choke the phenomenon, whereas the geometrical field increases more or less quickly according to the applied voltage shape. With the diffusion of space charge, the field will increase again up to  $E_c$ , according to applied voltage, and the dark period ends with the apparition of a new corona.

### **2.2.4 Leader**

Increasing the applied voltage, the secondary avalanches intensify and the vicinity of the high voltage electrode becomes a zone where the density of the streamer is very high. The mechanism of the corona to spark transition must involve heating of the air to a sufficient temperature for thermal ionization of the gas. Although each streamer is individually cold

and “less conducted”, their concentration will cause a local heating and an increase in temperature, which leads to the detachment of the electrons, i.e., thermal ionization of air. This will increase the conductivity in the discharge channel and form the leader (Fig. 2.2).

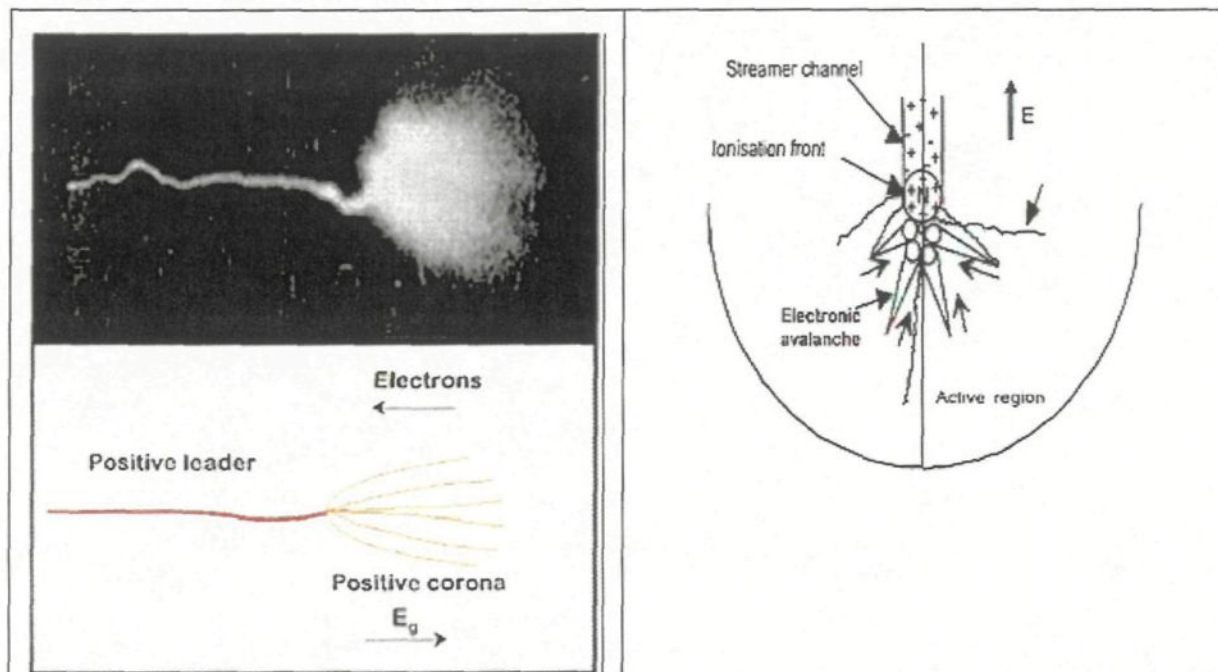


**Fig.2.2 Streamer-leader schematic representation [28]**

The leader contains a few negative ions and constitutes plasma of electrons and positive ions. The major part of potential of the HV rod is transferred to the end of the leader, so new coronas are able to start. These coronas have the same characteristics as the first corona and will lead to leader extension.

The ability of leader propagation through the gap depends on the field around the head and in the streamer zone in front of it. As the leader propagates, its head moves through the

gap space, together with the point of inception of new streamers and with streamer zone boundary. The earlier streamers and their space charge do not move forward. As a result, the elongating leader enters the charge-filled space.

### **2.2.5 Final jump**

The leader continues its propagation and the streamer coronas can reach the other electrode. The leader accelerates immediately after the streamer contact. The current rises suddenly and breakdown takes place [28].

## **2.3 Flashover on polluted surfaces**

### **2.3.1 General description**

Generally, the surface of insulators is covered with a layer of pollutants, which is accumulated since installation or the last cleaning operation. In some zones, the deposited layer will decrease dramatically the insulating strength of insulators and, under certain environmental conditions; result in flashover faults. These zones include either areas of high industrial density or the suburbs of large cities, installations near the sea, or exposed to strong winds coming from the sea, or close to deserts where the insulators are exposed to the strong winds transporting sand and salt.

Normally, the dry contamination layer does not endanger the power system operation. However, when the contamination layer is wetted due to condensation, frost, drizzle, fog, or onshore gales, etc., its conductivity will decrease dramatically. Sometimes this will cause flashover faults. Generally, the flashover process on polluted insulators includes several necessary steps as shown in Fig. 2.3, [34] [35].

### **Step 1**

When the contamination layer is wetted, a leakage current flows through it, due to its high conductivity. The value of leakage current depends on conductivity.

### **Step 2**

The leakage current will heat the insulator surface and cause the surface temperature to increase. Due to the shape of insulators, the current density on the surface is generally non-uniform. In the areas of high current density, the heating effect of current is greater and a local dry zone will appear in these areas.

### **Step 3**

The local dry zone will lead to the constriction of current. Then, the dry zone has a tendency to extend laterally until a complete dry band is formed and the current is interrupted.

### **Step 4**

The resistivity of the dry band is much higher than that of the wet contamination layer. The applied voltage will mostly drop along the dry band. If the voltage is high enough, the air around the dry band will be broken down and a partial arc will appear across it.

### **Step 5**

Depending on the conditions, the partial arc can evolve in two different ways: it may die out, or move laterally to find a more stable position corresponding to a shorter arcing distance.

### **Step 6**

If the applied voltage is high enough, the partial arc will extend longitudinally until it reaches the electrodes and causes a total flashover. In this case, the arc propagates on the surface of the electrolyte without the formation of a dry zone.

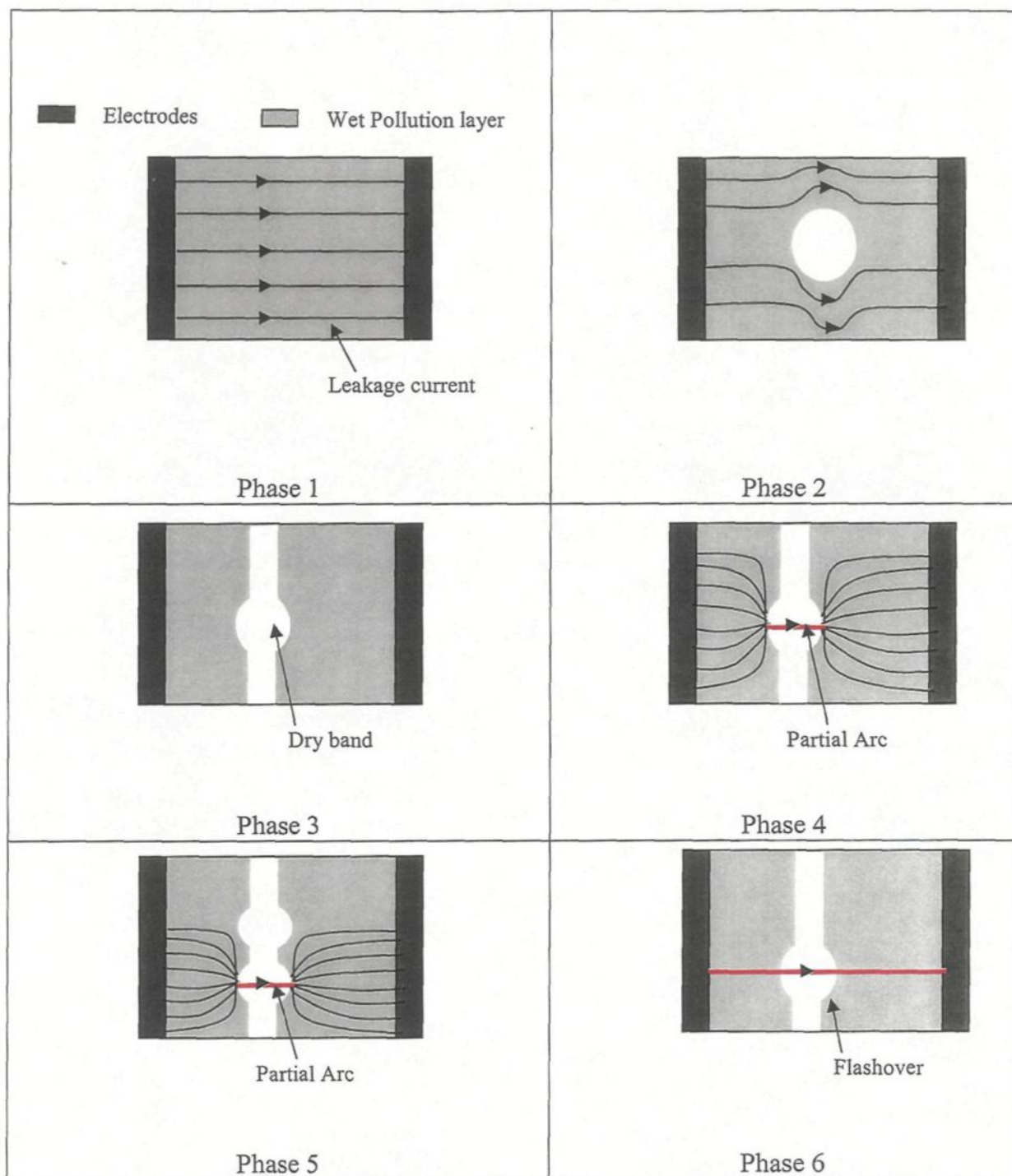


**Fig.2.3 Flashover process on polluted surface**

## 2.3.2 Modeling of arc on polluted insulators

Field and laboratory experimental studies are costly and time consuming, while mathematical modeling is one of the most efficient methods. Many efforts have been made to establish a mathematical model for predicting the flashover performance of polluted insulators [52].

### 2.3.2.1 DC models

Obenaus is the first person who quantitatively analyzed flashover on polluted surfaces [48]. The concept of his model is schematically given in Fig. 2.4, which consists of a local arc in series with the part of polluted surface that is not bridged by arc, and will be called residual resistance hereafter.

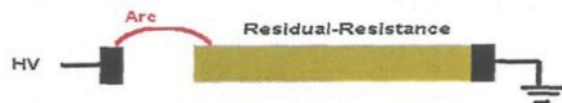


**Fig.2.4 Obenaus model of flashover on a polluted surface**

For this physical model, the circuit equation is:

$$U=U_e+U_{arc}+R(x).I \quad (2.1)$$

where,  $U$  is the applied voltage;  $U_e$  is the voltage drop on the electrode;  $R(x)$  is the residual resistance of the pollution layer, and  $I$  is leakage current;  $U_{arc}$  is the voltage drop along the arc column and it can be expressed as follows:

$$U_{arc} = AxI^n \quad (2.2)$$

where  $x$  is the length of local arc;  $A$  and  $n$  are the arc constants.

Then the Obenaus equation is:

$$U = U_e + AxI^n + R(x).I \quad (2.3)$$

As the leakage current  $I$  increases,  $U$  varies and yields a minimum value. This means that a minimum voltage is necessary to sustain a partial arc burning on a polluted surface. If the applied voltage is no longer adequate to sustain it, the arc will extinguish and flashover will not occur. As the arc length  $x$  varies from 0 to the insulator length  $L$ , this minimum voltage for sustaining the arc varies and yields a maximum value. This value corresponds to the critical flashover voltage [52].

Considering a uniform residual polluted layer, Neumarker developed this model and obtained [47]:

$$R(x) = r_x (L-x) \quad (2.4)$$

where  $L$  is the insulator length;  $r_x$  is the resistance per unit residual leakage length. Then, he calculated the critical flashover voltage of uniform-polluted insulator as:

$$\frac{L}{U_c} = \left( \frac{1}{A^{n+1} r_x^{\frac{n}{n+1}}} \right) \quad (2.5)$$

Wilkins [59] proved that the distribution of leakage current on a polluted surface is not uniform, due to the current concentration at the arc root. For the case of a narrow strip, he calculated the residual resistance with the following formula:

$$R(x) = \frac{1}{\pi \gamma_e} \left[ \frac{\pi(L-x)}{w} + 0.5 \ln \left( \frac{w}{2\pi r} \right) \right] \quad (2.6)$$

where L is the leakage distance of polluted insulator; x is the arc length; and w is the width of the polluted strip.

Under DC conditions, the voltage drop on electrodes is 840 V [58]. For insulators with a large diameter, some parallel arcs may appear simultaneously across the dry band. Then a correction-coefficient,  $b_{\text{eff}} = \frac{3L}{2N}$ , was considered for adaptation to the Obenaus model [9],

where N is number of parallel arcs.

### 2.3.2.2 AC models

Under AC voltage, the current passes through zero twice in each cycle and, consequently, the local arc will extinguish twice in each cycle, which renders complex the mathematical model. Several researchers developed models based on experimental results. Therefore, these models were summarized by Rizk [52] as experiment-based models.

Hurley [36] based his model on an empirically established relationship between the minimum voltage necessary to sustain an ac arc over a rod-rod gap of length  $x$  in series with a series resistance  $R_p$ , as follows:

$$U_{c_x} = \text{const.} \cdot x^{2/3} R_p^{1/3} \quad (2.7)$$

An interesting point in this model is that the minimum flashover voltage  $U_c$  was found to depend on both the leakage path  $L$  and the minimum arcing distance  $L_a$  of the insulator, so that:

$$U_c = \text{const.} \cdot r_p^{1/3} L_a^{2/3} L^{1/3} \quad (2.8)$$

AC arcs will re-ignite to a certain length from extinction in each half cycle when the voltage across the gap is higher than the recovery dielectric strength of air. From this point, Claverie and Procheron [6][7] empirically determined the relationship between the minimum arc re-ignition voltage and the arc current, as well as the arc length as follows:

$$U_{cx} = \frac{800x}{\sqrt{I}} \quad (2.9)$$

They also suggested an approximate expression for the arc voltage at the ac current peak:

$$U_{arc} = \frac{100x}{\sqrt{I}} \quad (2.10)$$

Guan *et al.* investigated the propagation of an AC arc on a polluted surface using a high-speed camera [33] and found that the arc develops only when it approaches the peak value of the applied voltage. In order to complete the flashover, a criterion called the arc recovery condition must be satisfied. They also experimentally determined the arc recovery conditions on polluted surfaces as follows:

$$V_m \geq \frac{k^* x}{I_m^{b^*}} \quad (2.11)$$

where  $k^*$ ,  $b^*$  are constants;  $V_m$  is the applied voltage; and  $I_m$  is the peak value of arc current [52].

## 2.4 Flashover of ice-covered insulators

The flashover on ice-covered insulators is still one of the most challenging problems of power systems in cold climate regions. This phenomenon has been investigated by many researchers, and a large number of practical and theoretical studies have been carried out in several laboratories. Reviews of these investigations were done in previous publications [14][13] and recent papers by an IEEE taskforce [10].

### 2.4.1 Description of the flashover on ice-covered surfaces

The flashover on ice-covered insulators is not only an electrical process but also thermal and electrochemical processes. The flashover process can generally be divided into 4 steps as follows [12]:

### **Step 1      Deposition of ice layer**

By a variety of conditions including hoar frost caused by condensation of vapor, in-cloud icing involving the freezing of super-cooled droplets in clouds or fog, and finally precipitation icing resulting from freezing rain, drizzle, wet snow, or dry snow, natural atmospheric ice is accumulated on insulator surfaces. During ice accretion, due to the heating effect of partial discharges or ice shedding from the insulators, several parts of the insulators, especially the areas near the electrodes, may be free of ice. These zones are referred to as air gaps.

### **Step 2      Formation of the water film**

It has been proven that the presence of a highly conductive water film on an ice surface is necessary for the occurrence of flashover. This water film can be produced by many factors, such as wet ice accretion, condensation, heating effect of the leakage current and partial arcs or, in many cases, by the rise in air temperature or sunshine. The high conductivity of the water film is caused by the rejection of impurities from the solid part toward the liquid portion of drops or droplets during solidification and by pollution of the water and ice surface by the products of corona discharge.

### **Step 3      Formation of local arcs across the air gaps**

Most of the applied voltage drops across the air gaps. If stress along the air gaps is high enough, several violet arcs will appear across them.

#### **Step 4 Propagation of local arcs and flashover**

If the applied voltage is high enough, a local arc can transform into a white arc and extend along the ice surface. Finally, when the white arc reaches a certain length, flashover occurs suddenly.

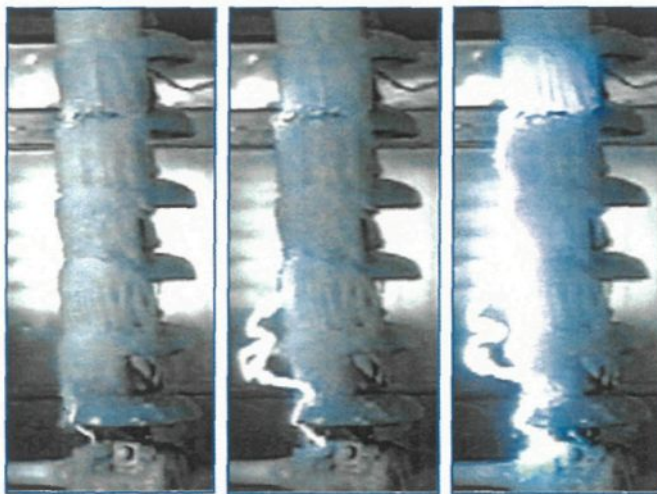


**Fig.2.5 Arc inception and development on an ice-covered insulator**

#### **2.4.2 Factors influencing the flashover voltage of ice-covered insulators**

The insulator parameters, the ice characteristics and the atmospheric conditions may influence the ac flashover voltage of ice-covered insulators.

### 2.4.2.1 Influence of insulator type and configuration

The performance of insulators under icing conditions depends not only on different icing conditions, but also on their shape and the materials of which they are made. One of the open problems in this area is the design of specialized types of insulators that are “anti-atmospheric icing”.

For the same materials and specifications, the short-space-shed insulators are more likely to flashover, and alternate sheds tend to show evidence of more satisfactory performance than uniform sheds [21].

For the same icing conditions for long-rod transmission insulators, the performance of the composite insulator is superior to IEEE standard insulators [4]. Also Wu *et al* [60] reported that the insulating performance of composite insulators, SiR (Silicone Rubber) and EPDM (Ethylene Propylene Diane Monomers), was superior to that of glass cap-pin insulator strings.

Under similar conditions, the probability of flashover of large diameter insulators is higher than the smaller ones, because the amount of ice accretion on an object is proportional to the surface exposed to super cooled droplets. Consequently, an insulator with a large diameter will accumulate more ice than a same-length, smaller-diameter

insulator. In terms of electrical performance, this means that large insulators will lose more of their leakage resistance than smaller ones [21].

The configuration of insulators has an obvious effect on their flashover voltage. With horizontal and V-string insulators, the possibility of ice bridging, and consequently flashover is reduced when compared to vertical insulators [1] [53].

#### **2.4.2.2 Influence of insulator length**

The flashover performance of short string of insulators covered with ice was studied by Farzaneh *et al* [13], Phan *et al* [50] and Kannus *et al* [42] independently. It was found that the flashover voltage of a short insulator string increased in a more or less linear fashion with the increase in insulator string length, up to 1 m.

Kawai [43] tested the flashover voltage of both long and short insulator strings covered with ice. No linear relationship between insulation strength and insulator length was revealed under mild icing conditions. The flashover voltage for an insulator unit was considerably lower for a long insulator string of 19 to 25 units than that for a short insulator string of 5 to 7 units. Due to complexity of the work and laboratory limitations, there is not any precise reference in the case of long insulators. Therefore, the flashover performance of ice-covered EHV insulators on a large scale needs further study.

### 2.4.2.3 Influence of ice type and density

Atmospheric ice accreted on structures such as insulators is different from that obtained by freezing of water, e.g., the ice of frozen lakes. Atmospheric ice results from a variety of conditions, including hoar frost caused by condensation of vapor, in-cloud icing involving the freezing of super-cooled droplets in clouds or fog, and finally, precipitation icing resulting from freezing rain, drizzle, wet snow, or dry snow.

Characteristics of ice vary depending on the environmental conditions, such as air temperature, wind velocity, water droplet size, and liquid water content.

Kuroiwa [45], Imai [40] and Oguchi [49] classified ice into three basic categories: hard rime; soft rime, and glaze. These types of ice have different appearance and density as presented in table 2.1.

**Table 2.1 Characteristics of ice formed on structures**

Type of ice	Density (g/cm <sup>3</sup> )	Appearance	Shape
Glaze	0.8-0.9	Transparent and clear	Cylindrical icicles
Hard rime	0.6-0.9	Opaque	Eccentric pennants in to wind
Soft rime	<0.6	White and opaque	Feathery and granular

Phan *et al* [50] found that for flashover studies there was no noticeable difference between the results obtained artificially and naturally.

Two regimes of icing were used by Farzaneh *et al* [22] for determining the flashover voltage of ice-covered insulators, i.e. the dry regime and the wet regime. Both hard rime and soft rime were grown under a dry regime. In this case, all the water droplets impinging on an insulator surface were completely frozen. There was no runoff water and icicles did not appear. In contrast, glaze is grown under a wet regime where icicles were formed around the insulator sheds. This type of ice deposition simulated ice accretion during freezing rain. The experimental parameters for dry-grown and wet-grown ice are listed in Table 2.2.

**Table 2.2 Experimental conditions for dry-grown and wet-grown ice [25]**

Type of Regime	Surrounding Temperature (°C)	Droplet Size (µm)	Wind Velocity (m/s)	Liquid Water Content (g/m <sup>3</sup> )
Dry	-12	15	3.3	6.8
Wet	-12	80	3.3	6.8

Different types of ice have different characteristics and different effects on the insulating strength of insulators. Therefore, a number of studies have been carried out on the minimum flashover voltage under soft rime, hard rime, and glaze conditions [21][44] and it was found that glaze with icicles is defined the most dangerous type of ice for flashover.

#### 2.4.2.4 Influence of amount of ice

Another parameter that affects the flashover voltage of ice-covered insulators is ice thickness. Due to non-uniformity of ice and complex geometry, the ice thickness on an insulator surface is difficult to measure. Therefore, several parameters were used to characterize the amount of ice on insulators. Some researchers used the ice weight on insulators to calculate the amount of ice [30] [54]. The withstand voltage of ice-covered insulators decreased and tended to saturation as the weight of ice increased. Farzaneh *et al* [21] [15] used the thickness of wet ice grown on a rotating monitoring cylinder as a reference parameter to determine the amount of ice. The relationship between this reference parameter and the ice weight per meter of insulator string, as well as the maximum withstand stress,  $V_{ws}/m$ , for IEEE standard insulators covered with ice, was determined, as shown in Fig. 2.6. It was found that the  $V_{ws}/m$  of insulators decreased with an increase in ice thickness, up to a 2.5 cm, and then remained constant with further increase in ice thickness. For different kinds of ice-covered insulators, the critical ice thickness level at which  $V_{ws}$  goes constant was found different. It is 2 cm for anti-fog insulators, 2.5 cm for IEEE standard and EPDM insulators, and 3.0 cm for post insulators. When the ice thickness exceeded 1.5 cm, the probability of flashover on transmission-line insulators rose considerably.

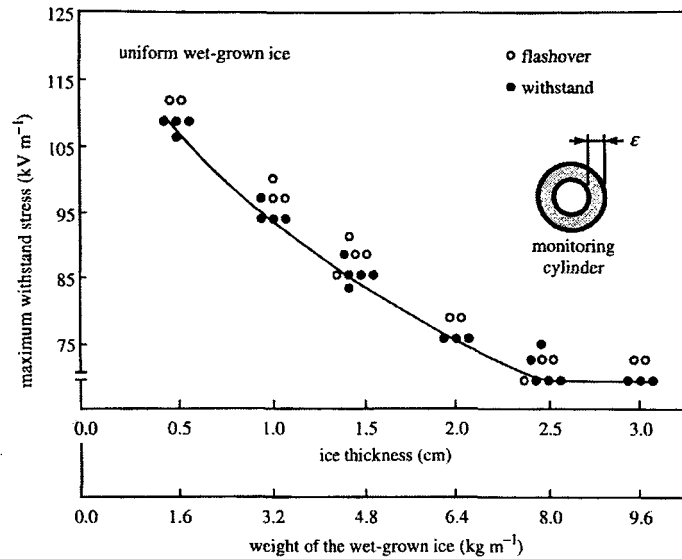


**Fig.2.6 Maximum withstand stress per meter of IEEE insulators as a function of the ice thickness on the monitoring cylinder and the corresponding weight of ice on 1 m of insulator string[21]**

#### 2.4.2.5 Influence of applied water conductivity

The pollutants in the atmosphere can increase the conductivity of atmospheric ice, which will consequently increase the leakage current of an ice-covered insulator and cause a decrease in insulating strength. The effect of applied water conductivity on the withstand voltage of ice-covered insulators was also studied at CIGELE [21] [22] [15]. The gradient of the maximum withstand voltage of an insulator decreased with an increase in the applied water conductivity, up to a value of  $80\mu\text{S}/\text{cm}$  (Fig. 2.7). After this level of water conductivity, the gradient of the maximum withstand voltage tended towards a saturation value.

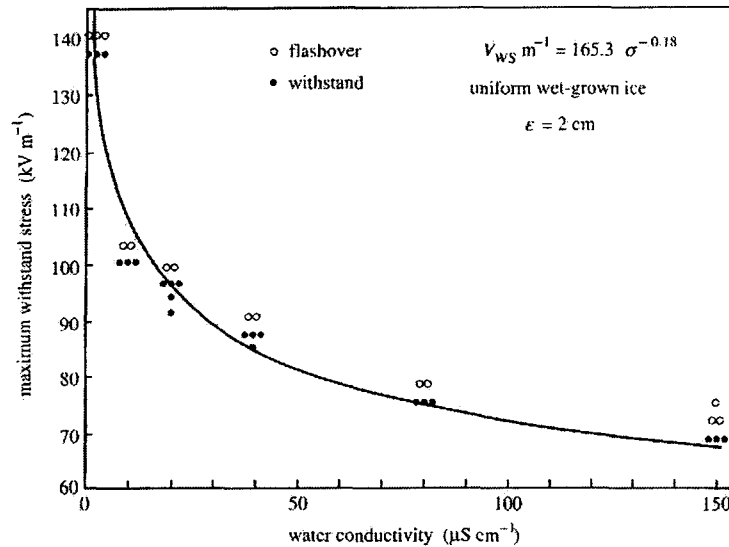


**Fig.2.7 Variation of  $V_{WS}$  of insulators as a function of applied water conductivity[13]**

The resistivity of the water producing the ice has a significant effect on leakage current, particularly when it drops from 90  $\Omega \cdot \text{m}$  to 9  $\Omega \cdot \text{m}$ . Under this condition, leakage current pulses start at the outset of icing and then increase rapidly [42]. The threshold value for the current of a white arc was observed to be approximately 18 mA during the flashover. When the leakage current was above this threshold, a white arc occurred on the insulator. The threshold value was independent of either the type of insulator or the type of ice. Furthermore, this value for the current of a white arc remained constant during periods of ice accumulation. Transition from a white arc to a flashover occurred when the leakage current rose above 120 mA for long-rod porcelain insulators, and 180 mA for a post-type porcelain insulator. This flashover threshold current was observed to be virtually equal to the maximum stable white arc [35].

### 2.4.3 Modeling of flashover on ice-covered insulators

Flashover on ice-covered insulators is a complex phenomenon. As mentioned above, it consists of four steps, and the accretion of an ice layer and formation of a water film generally take a long time. In other hand, laboratory simulation of flashover on ice-covered insulators requires expensive equipment, including a climate room. Therefore, field and laboratory studies of this phenomenon are costly and time consuming. Thus, mathematical modeling may be one of the most attractive ways to estimate the flashover performance of ice-covered insulators. Up to now, much effort has been put forth at CIGELE, finally leading to the development of a mathematical model [23][19].

In the case of ice-covered insulators, there are normally air gaps between the icicles and H.V electrode, in series with the accumulated ice, which has a relatively high surface conductivity. As mentioned above, the air gaps are caused by the heating effect of the discharge activities and ice shedding during accretion. A water film is formed on the ice surface by melting ice, as a result of a rise in air temperature, sunshine, the heating effects of corona discharge, and leakage current. This creates a situation similar to that of polluted insulators, i.e., dry bands in series with a wet pollution layer. Therefore, ice is considered to be a special type of pollution, and methods similar to those used for polluted insulators were used in the modeling of flashover on ice-covered insulators [23]. That is, the Obenaus model, as shown in Fig. 2.8.

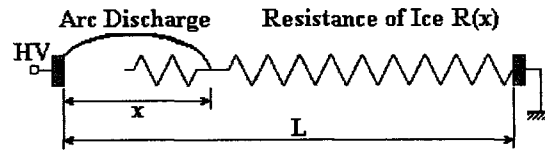


**Fig.2.8 Model for flashover on ice-covered insulators**

The circuit equation for this model is follows:

$$V_m = A \times I_m^{-n} + I_m R(x) + V_e \quad (2.12)$$

where  $V_m$  (V) is the peak value of applied voltage;  $V_e$  (V) is the electrode voltage drop of arc;  $x$  (cm) is the arc length;  $I_m$  (A) is the peak value of leakage current;  $R(x)$  ( $\Omega$ ) is the residual resistance of ice layer; and  $A$  and  $n$  are the arc constants.

For AC arcs, the arc electrode voltage drop,  $V_e$ , can be neglected and induced in the voltage drop along the arc [23], thus:

$$V_m = A \times I_m^{-n} + I_m R(x) \quad (2.13)$$

Under AC voltage, the current passes through zero twice in each cycle and, consequently, the local arc extinguishes and re-ignites twice. Therefore, not only Equation (2.12) but also the arc re-ignition conditions must be satisfied, which can be expressed as follows:

$$V_m \geq \frac{kx}{I_m^b} V \quad (2.14)$$

and the critical condition is:

$$V_m = \frac{kx}{I_m^b} V \quad (2.15)$$

where  $k$  and  $b$  are the arc re-ignition constants.

Studies have shown that when the insulator is completely covered with ice, the flashover voltage is lowest [20]. In this case, the ice layer can be simplified as a half cylinder [61] and the residual resistance can be calculated using the following formula [21]:

$$R(x) = \frac{1}{2\pi\gamma_e} \left[ \frac{4(L-x)}{D+2d} + \ln\left(\frac{D+2d}{4r}\right) \right] \quad (2.16)$$

where  $\gamma_e$  (in  $\mu S$ ) is the surface conductivity of the ice layer;  $L$  and  $D$  are the length and diameter of the insulator string, respectively;  $d$  is the thickness of the ice layer; and  $r$  is the arc root radius.

From Equations (2.12) and (2.15), the flashover voltage of ice-covered insulators can be calculated if all the parameters in Equations (2.12), (2.15), and (2.16) are determined. In previous work at CIGELE, these parameters were experimentally determined [23].

In order to determine the arc constants  $A$  and  $n$ , a simple geometry of flat-plane triangular ice sample was used (Fig. 2.8). This geometry ensures the formation of one

partial arc in a predetermined location and makes it easier to measure the voltage drop across it [23].

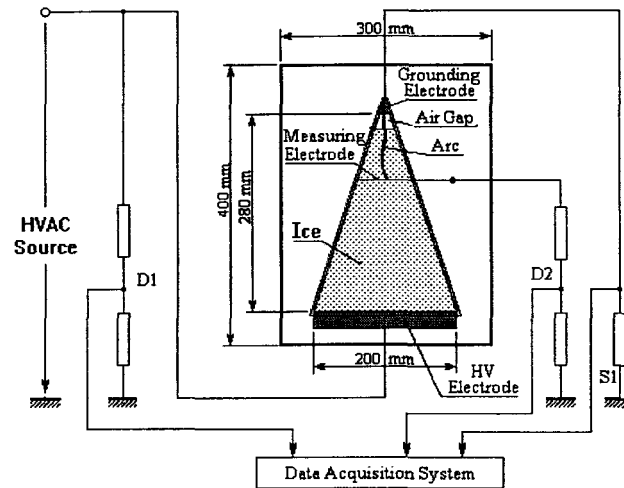


**Fig.2.9 Ice sample used for determining arc parameters [23]**

Two test methods were used for static and dynamic arcs, respectively [23]:

- 1) In the first method, an air gap with a constant width was made. A measuring electrode was installed at the ice surface at a given position. A voltage was applied to the HV electrode and raised at a constant rate until flashover occurred. The applied voltage and the voltage on the measuring electrode, as well as the leakage current were recorded simultaneously using a data acquisition system. In order to change the length of arc, a new sample was used and the measuring electrode was adjusted to a new position corresponding to the desired arc length. In this method, when the partial arc reached the measuring electrode, it did not stop but extended

continuously toward another electrode. Therefore, this method is proposed for measuring dynamic arc characteristics.

- 2) In the second method, an air gap between 1 and 7 cm wide was made. The measuring electrode was installed at the base of the air gap and the voltage was applied and raised until breakdown of the air gap. In this method, a steady arc is established only along the air gap. Therefore, this method is recommended for measuring static arc characteristics.

Using these methods, the voltage across the partial arc and the corresponding current was obtained by analyzing the waveform recorded by the data acquisition system (DAS). The typical waveforms of applied voltage ( $V_1$ ), voltage on the measuring electrode ( $V_2$ ), and leakage current ( $I$ ), are shown in Fig. 2.9. In each cycle, as  $V_1$  increased,  $V_2$  increased as well. When the air gap breakdown occurred ( $P_1$ ),  $V_2$  increased gradually. At the moment when the arc reached the measuring electrode ( $P_2$ ),  $V_2$  dropped suddenly. Due to the descending V-I arc characteristics, the lowest value of  $V_2$  appeared near the maximum current value. Therefore, it is easy to distinguish the moment when the arc reached the measuring electrode. Voltage  $V_2$ , at this moment, corresponds to the voltage across the arc.

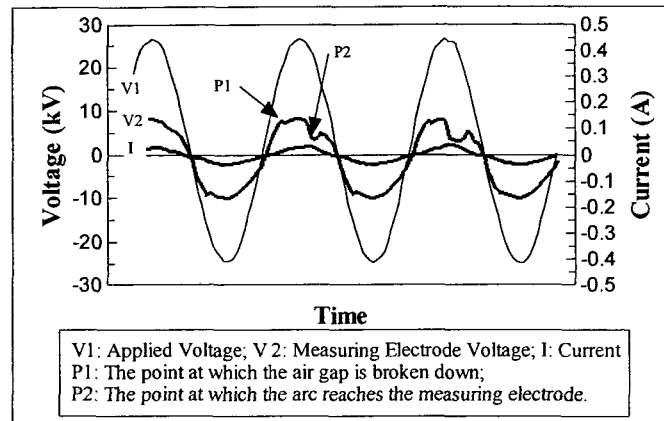


**Fig.2.10 Typical waveforms of applied voltage ( $V_1$ ), voltage on measuring electrode ( $V_2$ ), and leakage current ( $I$ ) [23]**

The E-I characteristics of the arc can be expressed as follows [23]:

$$E_{\text{arc}} = V_{\text{arc}} / x = AI^{-n}_m \quad (2.17)$$

where  $E_{\text{arc}}$  (V/cm) is the voltage gradient along the arc; and  $V_{\text{arc}}$  is the voltage drop along the arc.

Using different ice samples, made from water with various conductivities, the peak values of leakage current and the corresponding  $V_{\text{arc}}$  were measured. Figure 2.11 shows an example. The arc constants  $A$  and  $n$  can then be obtained by using regression on test results, as follows:

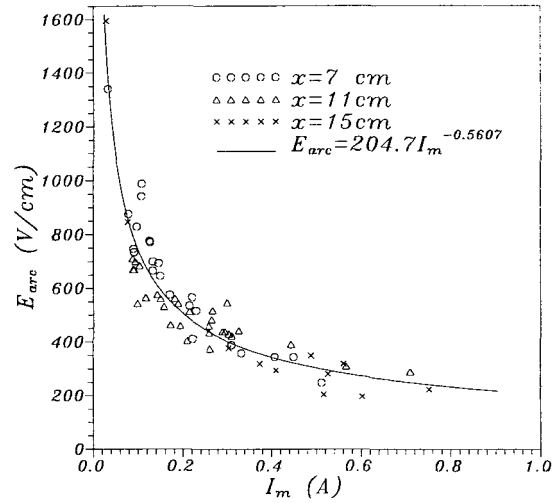


**Fig.2.11 E-I curve of arc on ice surface [23]**

$$A = 204.7 \quad (2.18)$$

$$n = 0.5607 \quad (2.19)$$

The arc re-ignition condition suggests a fact that, under the peak values of applied voltage  $V_m$  and leakage current  $I_m$ , the arc can re-ignite to a certain length  $x$ . Therefore, the critical relation between  $V_m$  and  $I_m$ ,  $x$  was determined and the arc re-ignition constants  $k$  and  $b$  were determined as [23] :

$$k=1118 \quad (2.20)$$

$$b=0.5277 \quad (2.21)$$

The relation between  $\gamma_e$  and the conductivity of water used to form the ice ( $\sigma$  in  $\mu s/cm$ ) was also determined as [23]:

$$\gamma_e = 0.0675 \sigma + 2.45 \quad (2.22)$$

The arc root radius was also measured using a high speed camera and it can be expressed as a function of leakage current [19]

$$r = \sqrt{\frac{I_m}{0.875\pi}} \quad (2.23)$$

All the necessary parameters in Equations (2.12), (2.15), and (2.16) have been determined. Therefore, this model can be used to predict critical voltage.

It should be mentioned  $A$  and  $n$ , and the arc re-ignition constant  $b$  are approximately independent from insulator dimensions [23] [16]. Chaarani studied the effects of insulator dimensions on the flashover performance of ice-covered insulators and reported that the arc re-ignition constant,  $k$ , depends on the insulator parameters [2].

As an application, this model was first applied to a short string of 5 IEEE standard insulators [61]. For 5 IEEE standard insulator units, the arc distance  $L$  and insulator diameter  $D$  are 80.9 cm and 25.4 cm, respectively. Considering the thickness of the ice layer ( $d$ ) of 2 cm, the calculated results were obtained, as shown in Fig. 2.12. It can be observed that there is good concordance between the flashover voltage calculated from the mathematical model and the experimental results, when the conductivity of water used to form the ice,  $\sigma$ , varies between 20 to 80  $\mu\text{S}/\text{cm}$ . When  $\sigma$  is very low or very high, there are some differences between the calculated and experimental results.

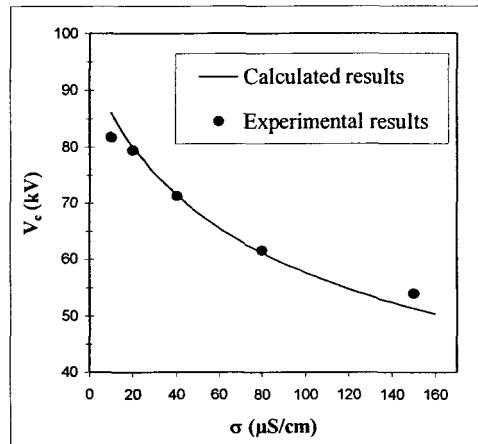


**Fig.2.12 Application of the model to 5 IEEE standard insulators [23]**

However, due to laboratory limitations, this model could not be applied to insulators longer than 1 m and therefore needs to be validated for application to long insulators [21] [12].

## 2.5 Conclusion

From the above literature review, it was observed that the flashover along an ice-covered insulator has received a great deal of attention from many researchers. A large number of studies have been carried out in several laboratories, especially in the research group CIGELE. The flashover performance of various insulators has been experimentally estimated in laboratories under icing conditions, and the affecting factors were also determined. Also, a series of fundamental studies has been done and a mathematical model

for predicting the flashover voltage of ice-covered insulators was successfully established. However, due to laboratory limitations, the flashover performance of full-scale EHV insulator covered with ice is not clearly revealed. As a result, this model was only validated for short insulators, which limited its use in engineering. Therefore, this Masters' research project was motivated by this shortcoming, to better understand the performance of long insulators under severe icing conditions, and improve the mathematical model for engineering applications.

## **CHAPTER 3**

# **EXPERIMENTAL FACILITIES AND TEST PROCEDURES**

## **Chapter 3**

# **Experimental Facilities and Test Procedures**

### **3.1 Introduction**

In order to achieve the objectives, an experimental study was systematically carried out in the HV laboratory of CIGELE on the flashover performance of long insulators. For this purpose, the atmospheric icing conditions were simulated and two test methods for evaluating the electrical performance of insulators under icing conditions were compared. This chapter introduces the laboratory facilities of CIGELE and the methods used in this study.

### **3.2 Facilities used in this study**

#### **3.2.1 Test insulators**

As mentioned in the literature review, much research has been done on short insulator strings. Therefore, this study aims to investigate the flashover performance of long insulators. For this purpose, a standard (STD) post-type porcelain insulator was selected (Fig. 3.1). This type of insulator is commonly used in Hydro-Quebec 735 kV substations. Three units of this type of insulator (full-scale for 735 kV systems) were installed vertically in a climate room at CIGELE.

One of major parameters influencing the flashover voltage of ice-covered insulator is dry-arcing distance. Thus, in order to determine the relationship between the flashover voltage of ice-covered insulator and its dry-arcing distance, 5 different lengths of dry-arcing distance, i.e., 1.39, 2.02, 3.07, 3.51, and finally 4.17 m which corresponds the full scale length for 735 kV systems, were selected for the tests in this study. The desired dry-arcing distance was obtained by changing the position of the ground electrode (Fig. 3.2).

### **3.2.2 Climate room**

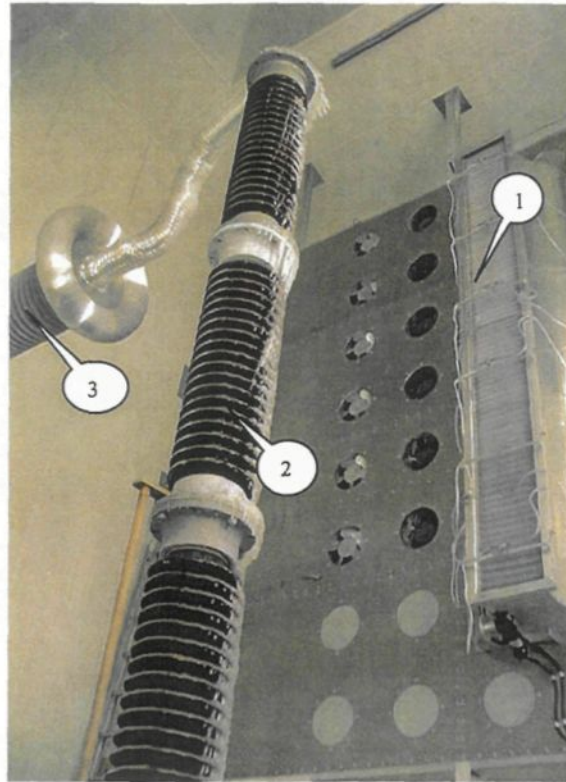
Scientific tests should be repeatable and comparable among researchers. Therefore, the tests were carried out in a laboratory, which makes it possible to control precisely the environmental conditions, such as temperature, humidity, ice-thickness, etc. In this study, all the tests were performed in one of the uniquely designed climate rooms at CIGELE (Fig. 3.3). This room, with a dimension of 6 m (w)  $\times$  6 m (l)  $\times$  9 m (h), is designed to study the performance of full-scale insulators. Its roof is designed to open to atmospheric conditions and allow exposure to natural precipitation, especially snow. The room is equipped with a water droplet generator and a cooling system, which makes it possible to form an ice layer on the surface of insulators.



**Fig.3.1 735 kV porcelain station post insulator  
with normal glaze and standard shed profile**



**Fig.3.2** Dry-arcing distance of ice-covered insulators is determined by the position of the Ground electrode



- 1 Water droplet generator
- 2 Insulator under testing
- 3 HV bushing

**Fig.3.3 Interior of the climate room**

### **3.2.3 Water droplet generator**

The water droplet generator is comprised of a system with 8 oscillating pneumatic nozzles and wind-producing fans. The type of nozzles is NO.SU12A (Fig. 3.4), and they are located in front of a diffusing honeycomb panel, designed to make the wind uniform. The spray angle was set at 45°.

The water droplet size is an important factor for determining the type of ice, and it depends on the pressure of the air and water fed in to nozzles. As mentioned above, glaze is the most dangerous type of ice to the power systems and, for that reason, it was chosen for this study. In order to produce glaze, the following parameters were used:

- The pressures of 10 psi for air and 80 psi for water were used. Under these pressures, the mean diameter of water droplet was  $80 \mu\text{m}$ . The water quantity was set to  $250 \text{ cm}^3/\text{min}$ . per nozzle.
- Wind velocity is another important factor affecting the type of ice. The wind was produced by 24 fans in a tapering box behind the nozzles. The fans may be mounted in a single or double stage arrangement, depending on the wind velocity desired. The velocity was adjusted by a PID controller in the range between 0 to 15 m/s. In this study, it was set to 3.3 m/s.

The specific design of the water droplet generator enables to change its position to form a very uniform ice layer on the test object mounted in any position (horizontal, vertical, or transverse).



**Fig.3.4 Pneumatic nozzle**

### 3.2.4 Cooling system

To simulate cold atmospheric conditions, an ammonia cooling system was used. This system is made up of a 316kJ/min. compressor and computer-controlled regulators, which allow to very rapidly reach air temperatures as low as  $-30^{\circ}\text{C} \pm 0.2^{\circ}\text{C}$ . The accuracy of temperature control is  $0.1^{\circ}\text{C}$ . In order to produce the glaze in this study, the environmental temperature was adjusted to  $-12^{\circ}\text{C}$  during the ice accretion period.

### 3.2.5 High Voltage System

In order to investigate the electrical performance of HV insulators, a high voltage power source is necessary. For the tests described herein, the high-voltage system consists of a 350-kV/700-kVA transformer and its associated 700-kVA voltage regulator (Fig. 3.5). It was specially designed for flashover tests on insulators under icing conditions, along with potential for further research under ice and contamination conditions. This system, with its

two-tap switch, has a minimum short-circuit current of 10 A at 130 kV, and maximums of 42 A at 240 kV and 32 A at 350 kV, satisfying the requirements of the international standard for pollution tests [41] . There are 5 different rates of increase for the output voltage, from 0 to 350 kV, regulated by the control unit.



**Fig.3.5 HV transformer with its associated regulator**

### **3.2.6 Data acquisition system**

The test data, including the applied voltage and leakage current, were monitored and recorded by a data acquisition system, which consists of a PC-compatible, high-speed data acquisition card and commercial software (LABVIEW) (Fig. 3.6). Figure 3.7 shows the interface programmed in LABVIEW. The results were presented in MS Excel Table formats for further processing and analysis. Considering the long duration of each

evaluation test, only the peak values of the leakage current was monitored at 5-second intervals.

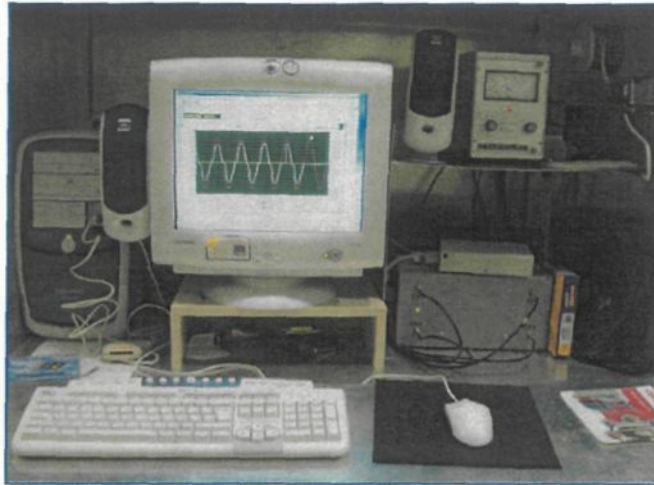


**Fig.3.6** Data acquisition system

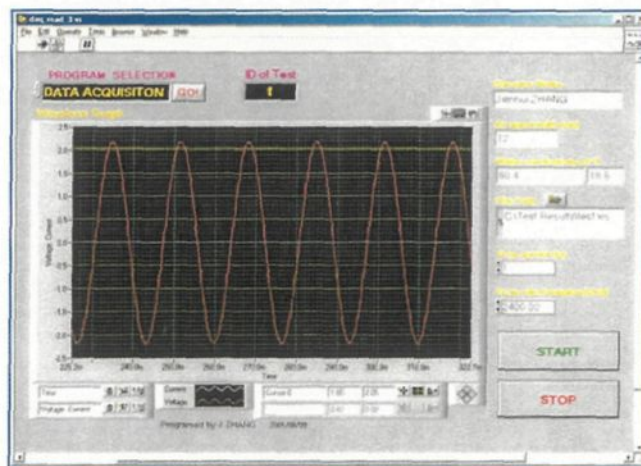


**Fig.3.7** LABVIEW interface designed for data gathering

### 3.2.7 Test circuit

The test circuit used in this study is shown in Fig. 3.8. After the ice was accumulated, the voltage was applied to the top electrode of the insulator. The applied voltage and the leakage current were measured using a voltage divider and a current shunt, respectively, and transferred to the data acquisition system.

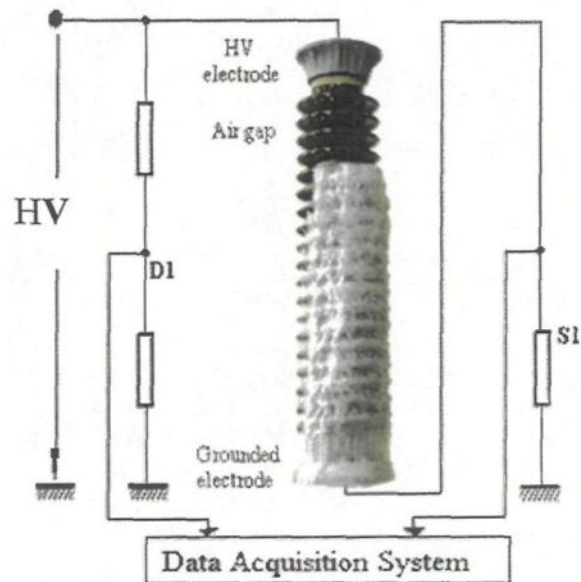


**Fig.3.8 Test circuit**

## **3.3 Test procedures**

### **3.3.1 Ice-thickness measurement**

As mentioned in Chapter 2, the amount of ice is an important factor influencing the flashover voltage of ice-covered insulators. The flashover voltage decreases with the increase in ice amount and tends to saturation when the insulator is completely covered with ice. In our study, the ice-thickness on a rotating monitoring cylinder was used as a reference parameter for characterizing the ice amount accumulated on the insulator. The diameter of this monitoring cylinder is 2.54 cm and it rotates at 1 rpm (Fig. 3.9). An ice-thickness of 15 mm on the monitoring cylinder is selected for this study, because this is a critical value of ice thickness to completely cover the windward side of the insulator and form a half-cylindrical ice layer. The ice thickness was measured at 5 different points on a monitoring conductor. Then, the average value was used as the ice thickness at this position of insulator (Fig. 3.10). The monitoring conductor was installed at different positions respectively, i.e., at the top, middle, and bottom of the insulator, to check the ice layer uniformity. The overall average value of all positions was then used to represent the thickness of the ice layer on the insulator (Fig. 3.11).

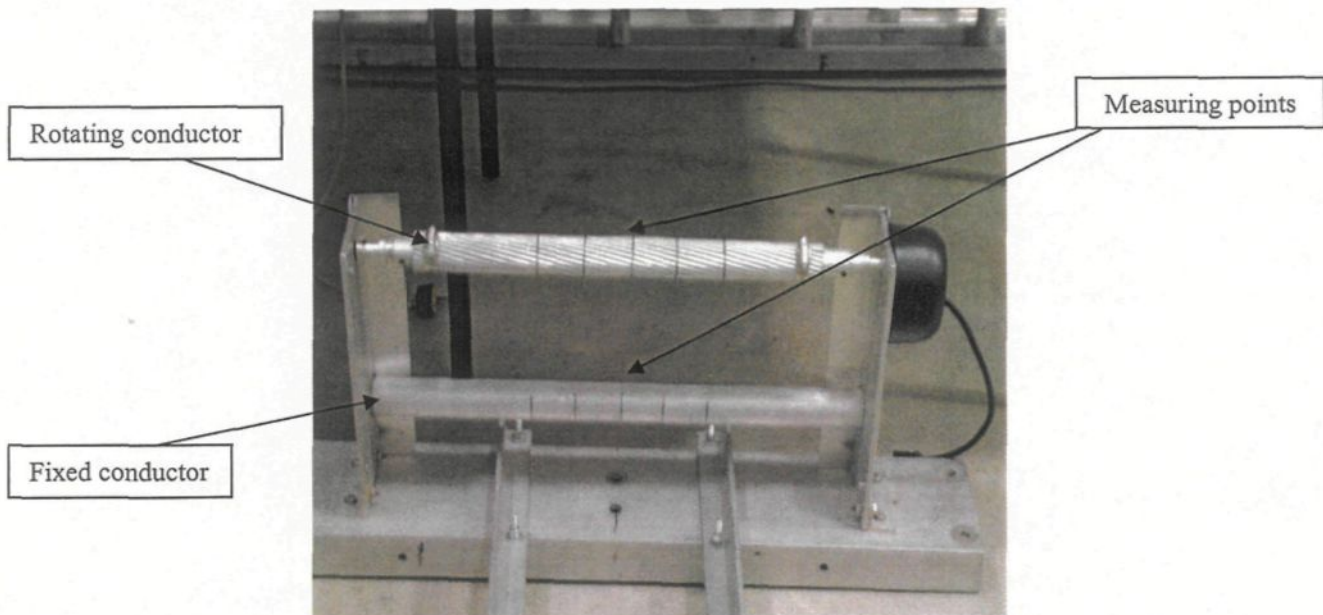


**Fig.3.9** Rotating and fixed monitoring cylinders

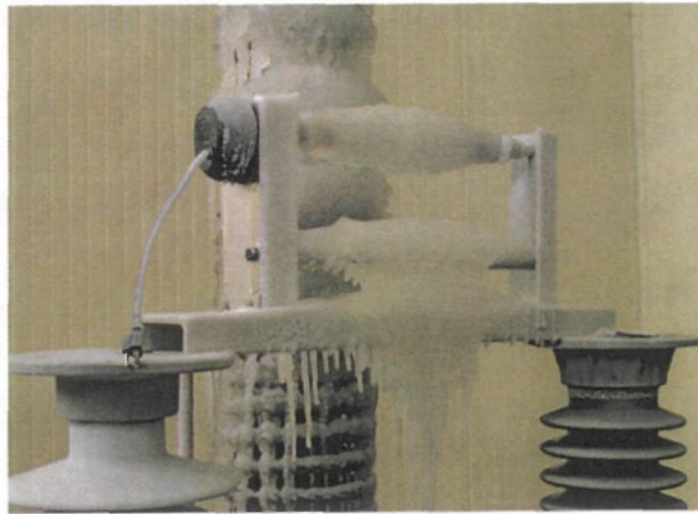


**Fig.3.10** Ice on monitoring conductors



**Fig.3.11 Monitoring conductors installed at different positions**

### **3.3.2 Evaluating the flashover voltage of ice-covered insulators**

According to a systematic investigation program undertaken jointly by Hydro-Quebec and UQAC in 1989, two test procedures for evaluating the electrical performance of ice-covered insulators, i.e. the icing regime and the melting regime, were developed at CIGELE. In this study, the effects of these two methods on the test results were investigated.

#### **3.3.2.1 Melting regime method**

The flashover of ice-covered insulators normally occurs when the ice melts due to an increase in ambient temperature or sunshine. In order to simulate this situation, a test

procedure called “melting regime” was developed at CIGELE. This procedure includes 4 basic sequences: ice accretion, curing, melting, and last evaluation of the maximum withstand voltage (Fig. 3.12).

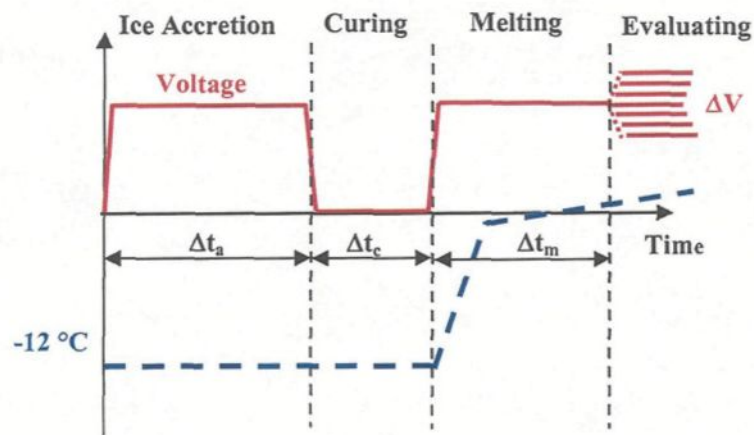


**Fig.3.12 Sequences of “melting regime” test procedure**

### Ice accretion sequence

In this sequence, wet-grown ice was built up on the vertically installed insulators, energized at approximately the equivalent of the service voltage used in Hydro-Quebec 735-kV substations. This type of ice is considered the most dangerous, since it is associated with the highest probability of flashover [14].

The density of ice accumulated on the insulators was determined by weight and volume measurements. The volume was obtained by immersing an ice sample in light mineral oil. The conductivity of the water feeding the nozzles was adjusted to a desired value by adding

sodium chloride to de-ionized water. The median volume diameter of the super-cooled droplets impinging on the insulators, at an average angle of about  $53^\circ$  compared to the vertical axis of the insulators, was measured by exposing a glass slide coated with a solution of Collargol to the flow of water droplets for a short period [32]. The samples were then examined under a microscope and the median volume diameter of these droplets was determined from the average diameter of approximately 1000 droplets. The intensity of the precipitation was determined from measurements of horizontal and vertical spray intensities using a pluviometer designed for standard tests [39]. This device is fitted with a divided collecting vessel, one horizontal and one vertical, the latter facing the spray. Last, the thickness of ice accumulated on the insulator, as mentioned above, was controlled by the monitoring cylinder.

Table3-1 summarizes the test parameters during the ice accretion sequence. Once the desired ice thickness on the monitoring cylinder is reached, 15 mm in this case, the water spraying system and the voltage applied to the insulator are turned off while the wind continues to blow at the same velocity of 3.3 m/s, whereupon the curing sequence begins.

**Table 3-1 Test parameters for the ice accretion sequence**

Test parameters	Parameters values
Air temperature	-12°C ( $\pm 0.2^\circ\text{C}$ )
Droplet size	80 $\mu\text{m}$
Incidence angle	53° ( $\pm 5^\circ$ )
Wind velocity	3.3 m/s
Ice thickness on monitoring cylinder	15 mm
Voltage gradient	105 kV/m for 30 $\mu\text{S/cm}$ (service voltage). 80 kV/m for 80 $\mu\text{S/cm}$

### **Curing sequence**

During this sequence, the temperature in the climatic chamber is maintained at  $-12^\circ\text{C}$  and the wind kept blowing at 3.3 m/s for a period of 20 min, to ensure that the liquid water present on the ice surface, inside the ice, and at the ice/insulator interface, is completely frozen. At the same time, it ensures a better adherence of the ice on the insulator surface. In addition, the curing sequence is highly representative of many icing episodes in natural conditions, where cold periods occur between ice accumulation and subsequent warm-up of the air temperature.

Once this sequence is completed, the fans and the cooling system are turned off and the insulators are re-energized at the same service voltage as that of the ice accretion sequence. This is followed by the melting sequence.

## **Melting sequence**

The melting sequence consists in raising the climate room temperature from sub-zero temperatures to a temperature near the melting point. The rate of increase in air temperature is a particularly important parameter and should be carefully controlled. In general, a low rate is associated with the worst conditions, since it promotes the formation of a highly conductive water film at the ice surface, with a relatively long duration [21] [17]. In the case of a high rate of increase (i.e. much faster than  $1^{\circ}\text{C}/\text{h}$ ), the highly conductive water film caused by melting quickly drips off, which decreases the ice surface conductivity and consequently raises the critical flashover voltage. In the present study, the air temperature in the climate room was increased in 2 steps by combining the opening of the door with an electrical heating system [11]. In the 1<sup>st</sup> step, the temperature was raised from  $-12^{\circ}\text{C}$  to  $-2^{\circ}\text{C}$  at a rate of about  $14^{\circ}\text{C}/\text{h}$  and, in the 2nd step, from  $-2^{\circ}\text{C}$  to  $+2.5^{\circ}\text{C}$  at a rate of about  $3.5^{\circ}\text{C}/\text{h}$ . Even though this rate is higher than  $1^{\circ}\text{C}/\text{h}$ , it was considered severe enough for the purpose of the present study.

## **Evaluating sequence**

This sequence consists in determining the maximum withstand voltage ( $V_{\text{ws}}$ ) of the insulators under a given ice thickness during the melting period, based on the method described in IEC 60507 [41], established for evaluating the electrical performance of polluted insulators, and on the processes developed in previous work [21][3]. The moment at which the voltage should be applied to the insulator is of great importance and should correspond to the critical moment when the probability of flashover is highest. This critical

moment typically coincides with the development of a water film at the ice surface. The brightness of the ice surface, the presence of water droplets at the tip of the icicles, and/or the steady increase in peak values of leakage current, over 15 mA, are all indications that the critical moment has been reached. Each flashover test was performed for one instance of ice accumulation on the insulators. The maximum withstand voltage,  $V_{WS}$ , was considered the maximum level of applied voltage at which flashover did not occur for a minimum of 3 tests out of 4, under similar experimental conditions. For each withstand test, the insulators were kept at the test voltage for a period of at least 15 min, to ensure that no flashover occurred during this period. The minimum flashover voltage,  $V_{MF}$ , corresponds to a voltage level  $\sim 5\%$  higher than  $V_{WS}$  at which 2 flashovers out of a maximum of 4 tests were produced.

### **3.3.2.2 Icing regime method**

The “melting regime” method is time consuming, as each test took about 5-7 hours. Also, judging the formation of water film is difficult and more or less subjective. For this reason, another test procedure, “icing regime”, was also developed at CIGELE, for evaluating the electrical performance of ice-covered insulators.

The test sequence for the procedure “icing regime” is presented schematically in Fig. 3.13. This procedure requires only two sequences, i.e., ice accretion and evaluation of the maximum withstand voltage. The ice accretion sequence is the same as that for the “melting regime”. Once the ice accretion sequence is completed, i.e., when an ice thickness

of 15 mm on the monitoring cylinder was obtained, the voltage applied to insulator,  $V_0$ , was turned off. Then, the icing process was stopped and the insulator was photographed and prepared for flashover tests. This period,  $\Delta t_0$ , took less than two minutes. After this short period, while a water film was still present on the ice surface, the voltage was immediately applied to the insulators and raised to an estimated test value,  $V_E$ . Thus, the evaluating sequence started and the maximum withstand voltage,  $V_{WS}$ , and the minimum flashover voltage,  $V_{MF}$ , were determined. In this procedure, every test took less than 2 hours.

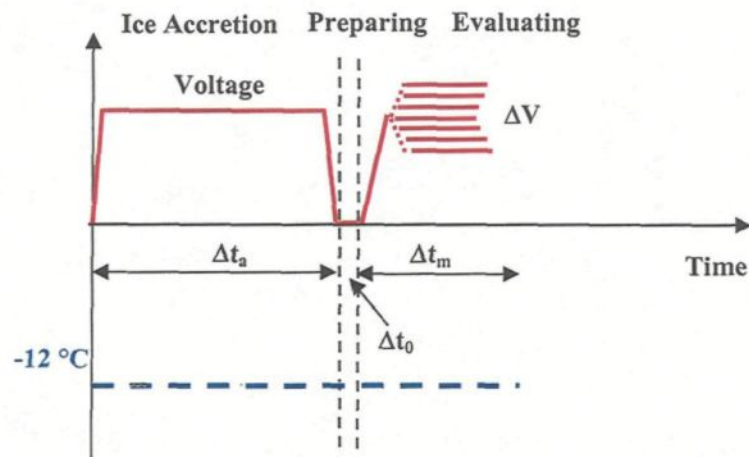


**Fig.3.13** Sequences of “icing regime” test procedure

## **CHAPTER 4**

# **EXPERIMENTAL RESULTS AND DISCUSSIONS**

# **Chapter4**

## **Experimental Results and Discussions**

### **4.1 Introduction**

Using the facilities and test procedures as described in Chapter 3, series of flashover tests were carried out. This chapter presents the experimental results obtained. First, the flashover process was observed carefully and is discussed. Then, the effects of experimental methods on the evaluated results are investigated and compared. Finally, the flashover performance of EHV standard porcelain post insulators was tested and the relationship between the minimum flashover voltage and the insulator dry arcing distance was determined.

### **4.2 Observation of flashover on EHV ice-covered insulators**

As mentioned above, when the ice thickness on the monitoring conductor reaches 15 mm, the icicles will bridge all the insulator sheds and an approximate half cylindrical ice layer is formed on insulator surface. This process takes about 70 min, and the ice accumulation process was photographed every 15 min. The following pictures show a typical accumulation of ice on a 2 m-long insulator.

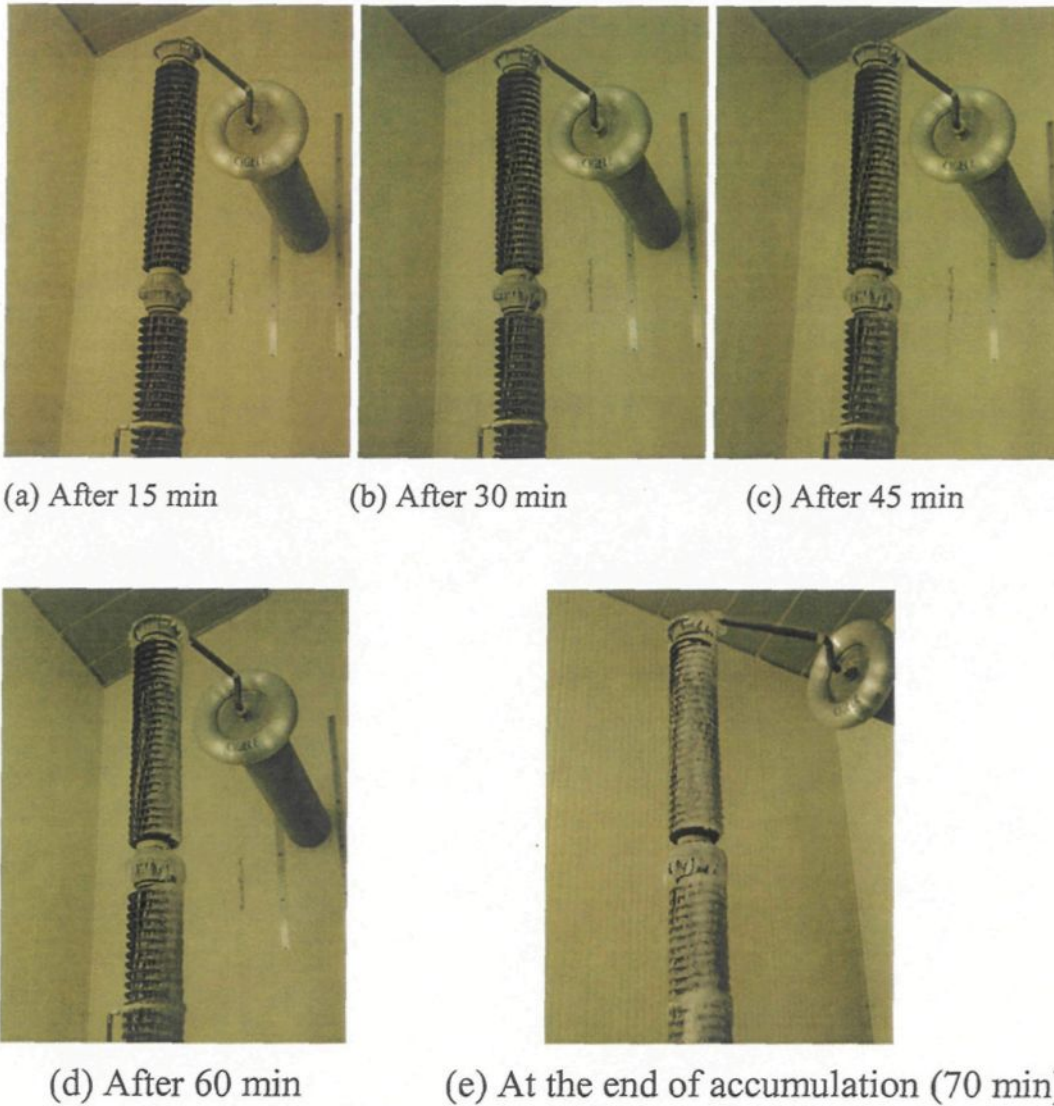


**Fig. 4.1 Accumulation of ice layer on insulator surface**

It can be observed that, after 30 min, the insulator sheds started to become bridged. Due to the larger space between the metallic electrode and the first or last shed of the top insulator, these spaces were not bridged and the partial discharge started at these areas, due to the applied voltage. These discharge activities cause the formation of air gaps. At the end of the accumulation period, the insulator side facing the wind was completely covered with

the ice, except for two major air-gaps: one at HV electrode and another between the last shed of the top electrode and metallic part. The divergent icicles were accumulated on the top metallic part of the top insulator. The top metallic parts of the second and third insulators were bridged completely by the ice.

After a short period of preparation (less than 2 min), the voltage was applied again and it was increased at a constant rate to the estimated flashover voltage. As the voltage increased, visible discharges were formed along the top air gap for a certain time, and then the visible discharges changed to a stable white arc across this air gap. Due to the low resistance of the arcs and the water film on the ice surface, most of the voltage drops across the second air gap. Consequently, a second white arc was formed along the second air gap, as shown in Fig.4.2.



**Fig.4.2 Two arcs along the air gaps**

Depending on the voltage applied, the top white arc may become elongated (Fig. 4.3). If the applied voltage is not sufficient for flashover, after certain time the white arc will extinguish due to the melting and shedding of the ice. If the voltage is high enough, the arcs will meet and flashover will occur.



**Fig. 4.3 Propagation of arcs on ice surface**

### **4.3 Comparison of evaluating methods**

As mentioned in the previous chapter, two methods were developed at CIGELE for evaluating the flashover performance of ice-covered insulators, i.e., the icing regime and the melting regime. In order to compare the effects of two test methods on the flashover performance of ice-covered insulators, using the same insulator and under the same experimental conditions, the maximum withstand voltage was determined.

The applied water conductivity was set at  $30 \mu\text{S}/\text{cm}$ . A portion of the standard station post insulator, with a dry arcing distance of 2.02 m, was tested with 15 mm of wet-grown ice. Under such icing conditions, the shed spaces are completely bridged with icicles and the leakage distance is dramatically decreased near to the dry arcing distance. The results are shown in Fig.4.4.

It can be observed that, for the melting regime, the maximum withstand voltage ( $V_{WS}$ ) is 195 kVrms. In Comparison to the service voltage of the insulator ( $\sim 210 \text{ kVrms}$ ),  $V_{WS}$  is equal to 0.93 p.u, indicating that the maximum withstand voltage of the insulators under the test conditions is lower than the service voltage by 7%.

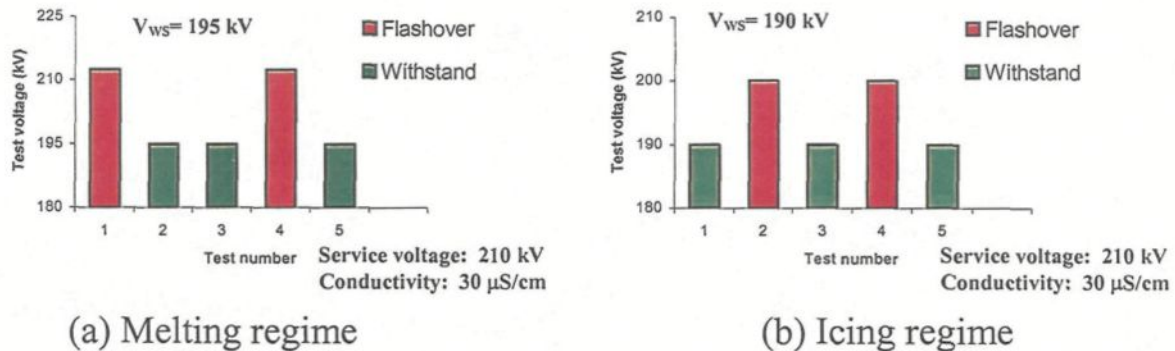


**Fig.4.4 Test results obtained on the STD post insulator covered with 15 mm of ice and with an arcing distance of 2.02 m**

For the icing regime, the maximum withstand voltage ( $V_{WS}$ ) is 190 kVrms. In comparison to the results in the “melting regime” procedure, the difference between them is less than 3%. The similar results have been reported for 1m ice-covered insulators[8]. Therefore, the  $V_{WS}$  for these two procedures can be considered as the same. Both the

melting and icing regime methods are developed for evaluating the flashover performance of ice-covered insulators in laboratories.

However, it should be mentioned that it is important to keep the water film on the ice surface when the evaluating sequence starts in the “icing regime” method. Otherwise, if the water film is completely frozen when the evaluating sequence starts, the  $V_{WS}$  would obviously increase. Therefore, the preparation period should be short enough to satisfy this condition. In this study, this period was kept shorter than 2 minutes.

#### **4.4 Experimental results**

In order to save time, the icing regime method was selected to investigate the flashover performance of EHV insulators covered with ice, and to determine the relationship between the maximum withstand voltage,  $V_{WS}$ , and the dry arcing distance of insulators.

Two different water conductivities were used to form the ice, i.e. 30  $\mu\text{S}/\text{cm}$  and 80  $\mu\text{S}/\text{cm}$  (at 20°C). The former was selected because the conductivity of natural atmospheric ice in Quebec was found to be around this value. However, due to the limited transformer output voltage, only three dry arcing distances, i.e. 1.39, 2.02 and 3.07m, were tested. In order to investigate the variation of flashover voltage with insulator length, up to the full scale of insulators, the water conductivity was increased to 80  $\mu\text{S}/\text{cm}$ . At this conductivity level, 5 dry arcing distances, i.e., 1.39, 2.02, 3.07, 3.51 and 4.17 m, were tested. The last one corresponds to full scale insulators, as typically used in Hydro-Quebec 735 kV systems.

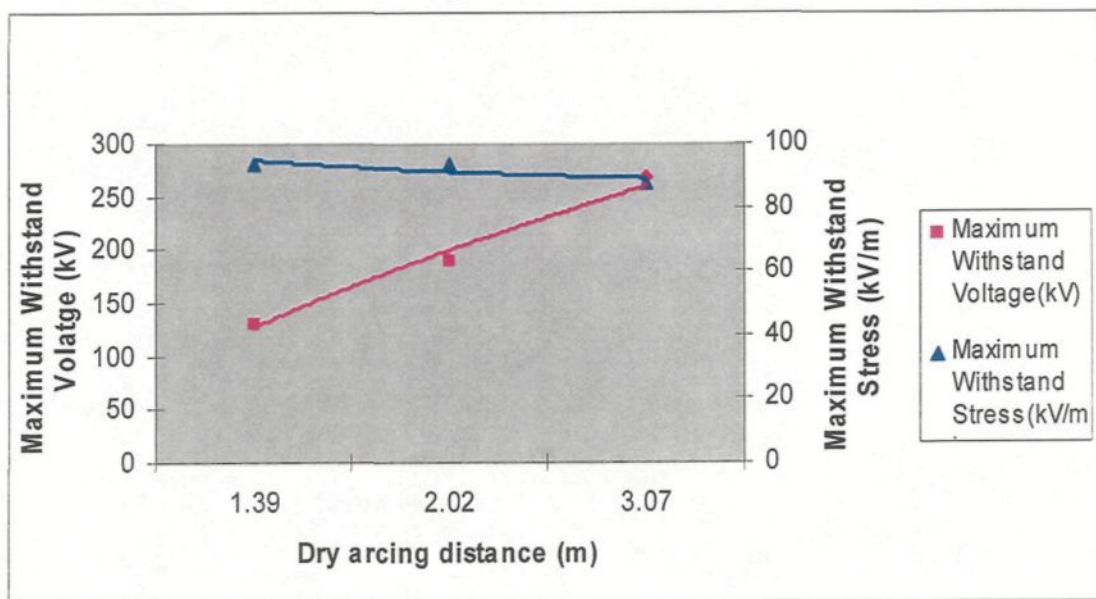
The water conductivity was adjusted by adding NaCl to the de-ionized water and then measured and calibrated to the value at 20 °C.

Table 4.1 and Fig. 4.5 show the results obtained at 30  $\mu\text{S}/\text{cm}$  water conductivity.

**Table 4.1 Test results for different dry arcing distances at 30  $\mu\text{S}/\text{cm}$**

L (cm)	Test voltage (kV) and result							$V_{MF}$ (kV)	$V_{WS}$ (kV)
	138	145	138	138	131	131	131		
139	W	F	F	F	W	W	W	138	131
202	W	F	F	W	W	-	-	200	190
307	F	F	W	W	F	W	W	285	270

Note F = Flashover; W = Withstand



**Fig.4.5  $V_{WS}$  as a function of dry arcing distance ( $\sigma = 30 \mu\text{S}/\text{cm}$ )**

It may be noted that  $V_{ws}$  increases with the increase in insulator dry arcing distance.

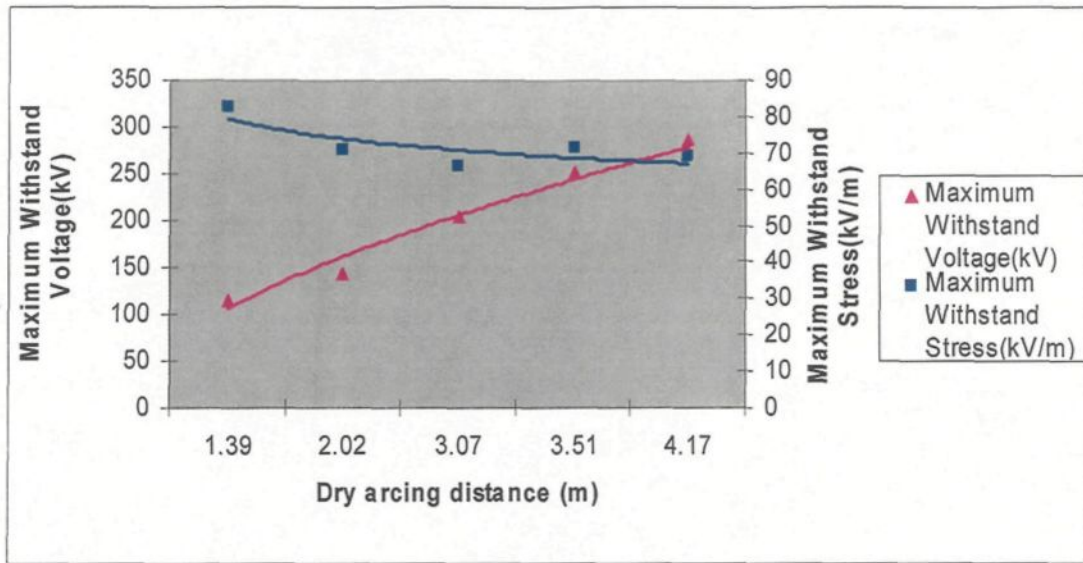
However, the withstand stress slightly decreases with an increase in insulator dry arcing distance, which suggests that the maximum withstand flashover voltage increases slightly non-linearly with the increase in insulator dry arcing distance.

Table 4.2 and Fig. 4.6 show the results obtained at  $80 \mu\text{S}/\text{cm}$  water conductivity, which corresponds to that of tap water in Quebec.

**Table 4.2 Test tests for different insulator lengths ( $80 \mu\text{S}/\text{cm}$ )**

L (cm)	Test voltage (kV) and result											$V_{MF}$ (kV)	$V_{ws}$ (kV)
139	110 W	115 W	120 F	120 W	120 F	115 W	115 W	-	-	-	-	120	115
202	150 F	143 W	150 F	143 W	143 W	-	-	-	-	-	-	150	143
307	240 W	240 F	240 F	228 F	216 W	216 F	204 W	204 W	216 F	204 F	204 W	216	204
351	252 W	252 W	266 W	266 F	252 W	266 W	266 F	-	-	-	-	266	252
417	272 F	256 W	272 W	272 W	288 W	288 W	304 F	288 W	304 F	-	-	304	288

Note F = Flashover; W = Withstand



**Fig.4.6**  $V_{WS}$  as a function of dry arcing distance ( $\sigma=80 \mu\text{S}/\text{cm}$ )

As was the case for  $30 \mu\text{S}/\text{cm}$ , the  $V_{WS}$  increased with an increase in the dry arcing distance, while the withstand stress decreased slightly. This decrease in stress may be related to different breakdown theories for short and long-distances. For short distances (i.e. less than 1m), the breakdown can be described by the streamer theory, but for long distances, it can be described by the leader theory. The leader theory explains the breakdown of long air gap as follows [28]: as the streamer extends, large number of charged particles flows to the electrode through the steamer channel. At the root of the streamer, the density of ions is so high as to result in the thermal ionization, and the leader is formed here. The conductivity of the leader is very high and it functions like an extension of the electrode. Therefore, the electric field strength will increase, which results in the decrease in breakdown voltage of long air gaps and the consequent non-linearity of breakdown voltage of air gap as its length. The flashover of long insulators covered with

ice is caused by leader discharge and may be explained by this theory. Therefore, the withstand stress decreases with an increase in the dry arcing distance.

## **4.5 Conclusions**

Using a post type insulator, a series of tests was carried out at the HV laboratory of CIGELE, to investigate the electrical performance of an EHV insulator covered with ice. The maximum withstand voltage ( $V_{ws}$ ) was measured using the icing and melting regimes. The results show that both test procedures are valid for evaluating the electrical performance of insulators under icing conditions. Using the icing regime method, the relationship between the maximum withstand voltage of ice-covered insulator and its dry arcing distance was determined. It was found that the  $V_{ws}$  increases in a slightly non-linear manner with an increase in insulator dry-arcing distance.

## **CHAPTER 5**

# **MODELING OF FLASHOVER ON ICE-COVERED INSULATORS**

## Chapter 5

# Modeling of Flashover on Ice-Covered EHV Insulators

### 5.1 Introduction

The field investigation and the laboratory studies for determining the flashover performance ice-covered insulators are generally costly and time consuming. Therefore, the mathematical model is probably one of the most interesting ways of estimating the critical flashover voltage of ice-covered insulators. As mentioned in Chapter 2, a mathematic model (Equations (2.12), (2.15) and (2.16)) has been developed at CIGELE for this purpose, and was successfully applied to short insulator strings covered with ice.

However, when this model is applied to an insulator string longer than 1 m, the error between the results calculated from the model and those obtained in laboratory increases markedly. The comparison between the calculated results and the experimental results for the applied water conductivities of 30 and 80  $\mu\text{S/cm}$  is shown in Tables 5.1 and 5.2, as well as Figs. 5.1 and 5.2, respectively. It should be noted that experimental results present the minimum flashover voltage ( $V_{MF}$ ) of ice-covered insulators, while the calculated results give their critical flashover voltage ( $V_C$ ). However, these two voltages are comparable,

since the difference between them is less than 2% for ice-covered insulators under AC conditions. It may be observed that average error is 14 %, and the maximum error is more than 19 %, which is not acceptable for engineering use. Therefore, this model needs to be improved for application to EHV insulators.

**Table5.1 Comparison between the experimental and calculated results  
( $\sigma = 80\mu\text{S/cm}$ )**

Dry arcing distance (m)	Experimental results (kV)	Results from existing model (kV)	Error (%)
1.39	120	97	19.2
2.02	150	135	10.0
3.07	216	199	7.9
3.51	266	226	15.0
4.17	304	266	12.5

**Table5.2 Comparison between the experimental and calculated results  
( $\sigma = 30\mu\text{S/cm}$ )**

Dry arcing distance (m)	Experimental results (kV)	Results from existing model (kV)	Error (%)
1.39	138	118	14.5
2.02	200	165	17.5
3.07	285	243	14.7

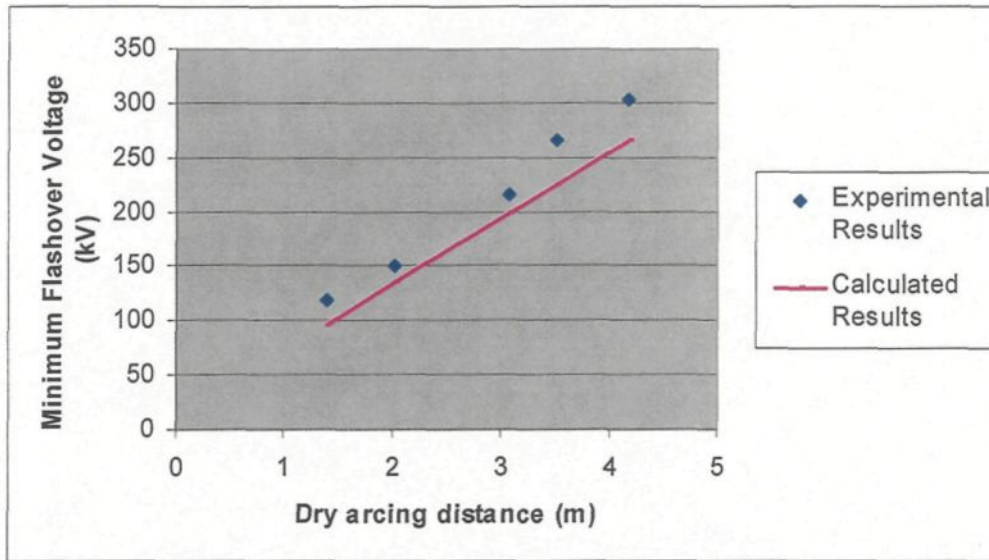


**Fig.5.1 Comparison between the experimental and calculated results  
( $\sigma = 80\mu\text{S}/\text{cm}$ )**

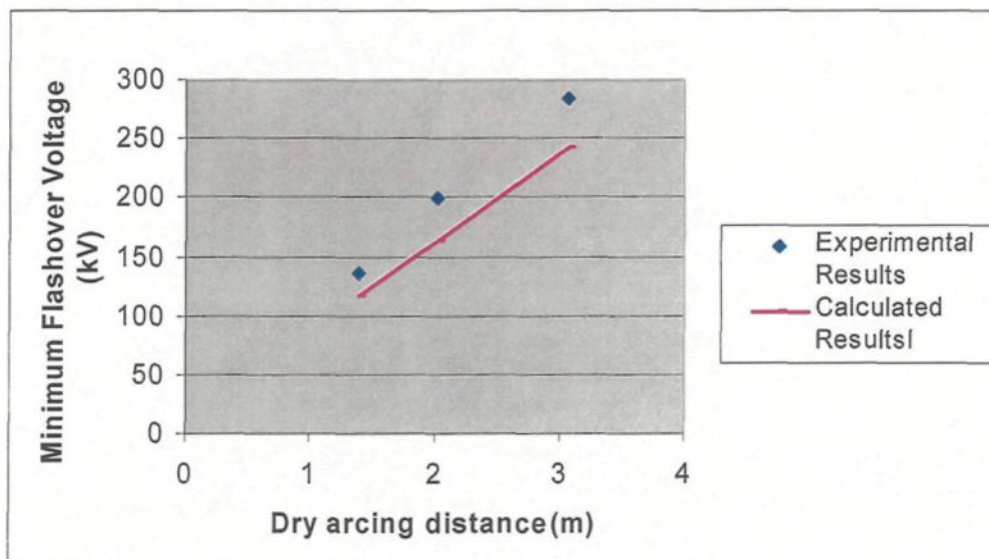


**Fig.5.2 Comparison between the experimental and calculated results  
( $\sigma = 30\mu\text{S}/\text{cm}$ )**

## 5.2 Improvement of the existing model

One of the important factors that influence the calculated minimum flashover voltage is the residual resistance of the ice layer. This resistance is influenced by the current distribution [58]. In the existing model, the flashover was considered as one local arc in series with the residual ice layer and, therefore, the residual resistance was calculated by Equation (2.16). In fact, from the flashover tests in this study, it was observed that, for insulators longer than 1 m, there usually were two arcs during flashover process: one near the HV electrode and another at lower part of the insulator (Fig. 5.3). If the applied voltage is high enough, these two major arcs will elongate, and finally meet to complete the flashover.



**Fig.5.3 Two arcs on insulator**

Therefore, the flashover on ice-covered insulators longer than 1 m should be modeled by double arcs in series with the residual ice layer (Fig. 5.4).

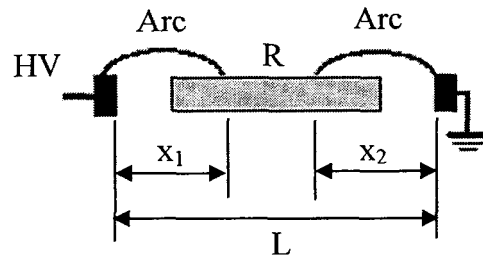


**Fig.5.4 Double arcs model**

In this case, the calculation of residual resistance should consider the current concentration at two arc roots. In fact, the model can be equivalently split into two parts, as shown in Fig. 5.5.

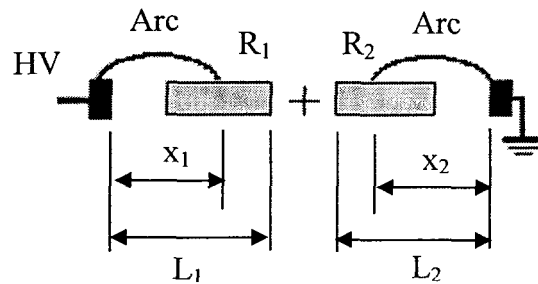


**Fig.5.5 Equivalent model**

where  $L_1 + L_2 = L$ ;  $x = x_1 + x_2$  is the total length of the local arc. From Equation (2.16), the residual resistance of the ice layer can be expressed as follows:

$$R(x) = R_1(x_1) + R_2(x_2) \quad (5.1)$$

where

$$R_1(x_1) = \frac{1}{2\pi\gamma_e} \left[ \frac{4(L_1 - x_1)}{D + 2d} + \ln\left(\frac{D + 2d}{4r}\right) \right] \quad (5.2)$$

$$R_2(x_2) = \frac{1}{2\pi\gamma_e} \left[ \frac{4(L_2 - x_2)}{D + 2d} + \ln\left(\frac{D + 2d}{4r}\right) \right] \quad (5.3)$$

Thus

$$R(x) = \frac{1}{2\pi\gamma_e} \left[ \frac{4(L - x)}{D + 2d} + 2\ln\left(\frac{D + 2d}{4r}\right) \right] \quad (5.4)$$

where  $\gamma_e$  (in  $\mu\text{S}$ ) is the surface conductivity of the ice layer;  $L$  and  $D$  (both in cm) are the length and diameter of the insulator, respectively;  $d$  (in cm) is the thickness of the ice layer; and  $r$  (in cm) is the arc root radius.

Therefore, the equation for this circuit model can be expressed as follows:

$$V_m = AxI_m^{-n} + I_m R(x) \quad (5.5)$$

where  $x = x_1 + x_2$  (in cm) is the total length of the two arcs;  $V_m$  (in V) and  $I_m$  (in A) are the peak values of applied voltage and leakage current, respectively;  $A$  &  $n$  are the arc constants; and  $R(x)$  (in  $\Omega$ ), is the electrical resistance of the part of the ice not bridged by the arcs.

Also, under AC conditions, in order to maintain an arc propagating on a dielectric surface, not only Equation (5.5) but also the arc re-ignition conditions, which can be expressed by Equation (2.15), must also be satisfied. The arc re-ignition condition represents that, under applied voltage  $V_m$  and the current  $I_m$ , the arc can reach length  $x$  after its previous extinction.

From Figs.5.1 and 5.2, it can be observed that all the experimental points are above the calculated results. The arc constants  $A$  and  $n$ , as well as the arc re-ignition constant  $b$ , are independent from insulator dimensions, while the arc re-ignition constant ' $k$ ' is affected by the insulator parameters, such as insulator diameter [3]. On the other hand, in the existing model the value of  $k$  and  $b$  were determined using a small triangular ice sample, and were not validated with long insulators. Therefore, the difference between the experimental results and those calculated from the existing model suggested that the arc re-ignition constant ' $k$ ' in Equation (2.15) should be increased. Based on the experimental results of this study, it was found that the value of  $k$  should be modified to:

$$k = 1,300 \quad (5.6)$$

for the insulators tested. Thus, the mathematical model, i.e., Equations (2.15), (5.4), and (5.5) can be used to predict the critical flashover voltage of EHV insulators under icing conditions.

These equations are complex and have no analytic solution. A numerical method was used to solve it, and the MATLAB program was developed for this purpose. Figure 5.6 shows the interface of the program. In this program, by entering the input parameters such as the applied water conductivity, the diameter and length of the insulator, as well as the ice thickness, the critical flashover voltage of this insulator under icing conditions can be calculated and displayed on the interface. Meanwhile, the critical leakage current and the critical arc length can also be calculated.

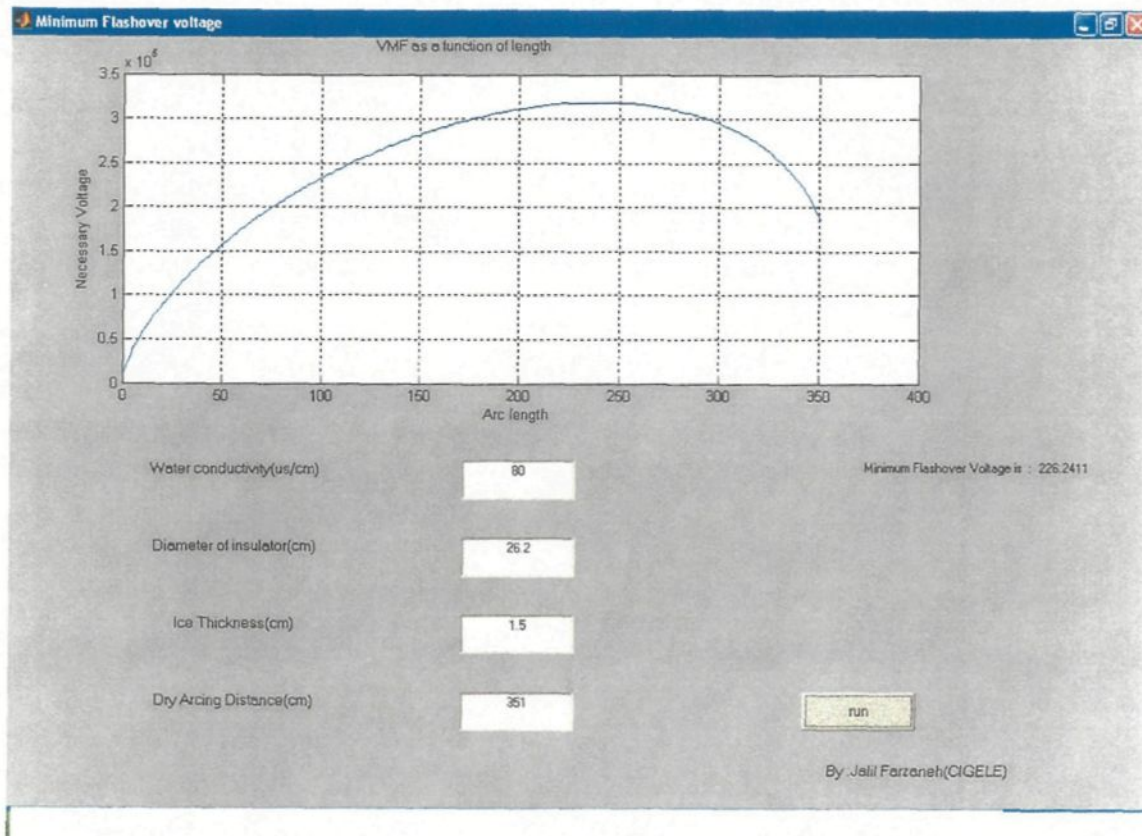


**Fig.5.6** The interface of improved model

### 5.3 Validation of the improved model

The model was validated by the experimental results obtained with standard porcelain post insulators for two different conductivities, 80 and 30  $\mu\text{S/cm}$ . In the calculation, the ice thickness was set to 15 mm. Tables 5.3 and 5.4, as well as Figs. 5.7 and 5.8, show the experimental results and the calculated results for conductivities of 80 and 30  $\mu\text{S/cm}$  respectively. It may be noted that there is good concordance, in view of engineering applications, between the experimental results and those calculated from the improved model. The maximum error is  $\sim 6.7\%$ .

**Table5.3 Comparison of experimental results and those from the improved model**

**for the STD porcelain post insulator ( $\sigma = 80 \mu \text{ S/cm}$ )**

Dry arcing distance (m)	$V_C$ from the model ( $\text{kV}_{rms}$ )	$V_{MF}$ from experiments ( $\text{kV}_{rms}$ )	Difference (%)
1.39	118	120	-1.7
2.02	160.8	150	6.7
3.07	230	216	6.1
3.51	260	266	-2.6
4.17	303.5	304	-0.2

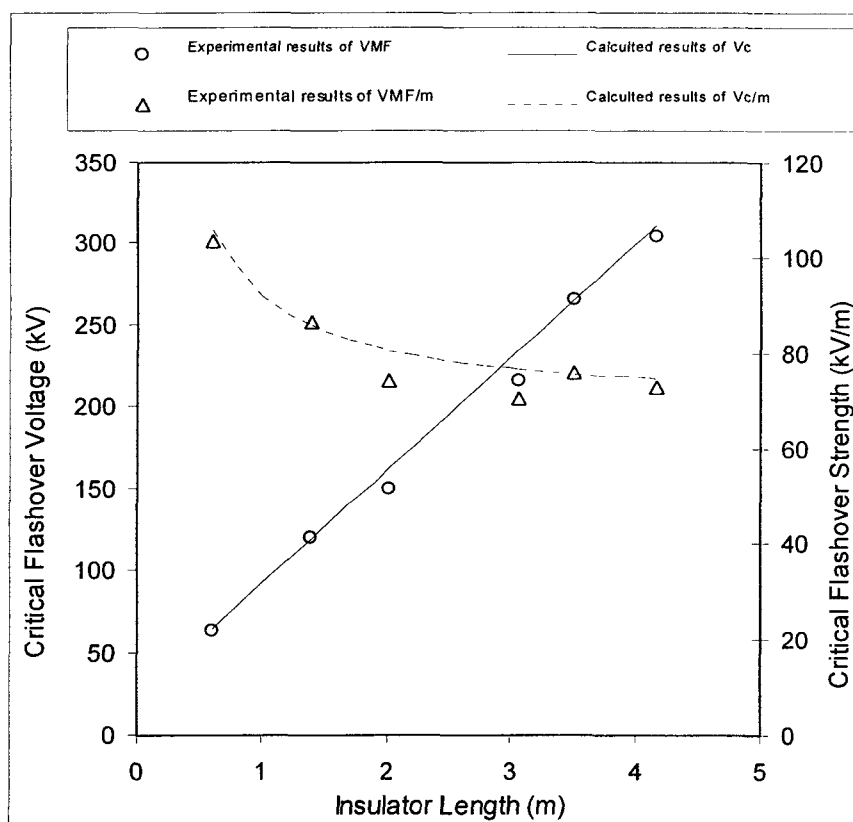


**Fig.5.7 Experimental results and those calculated from the improved model ( $\sigma = 80 \mu \text{ S/cm}$ )**

**Table5.4 Comparison of experimental results and those from the improved model for the STD porcelain post insulator ( $\sigma = 30 \mu \text{ S/cm}$ )**

Dry arcing distance (m)	$V_C$ from the model ( $\text{kV}_{\text{rms}}$ )	$V_{\text{MF}}$ from experiments ( $\text{kV}_{\text{rms}}$ )	Difference (%)
1.39	146	138	5.79
2.02	197.16	200	-1.42
3.07	282.26	285	-0.96

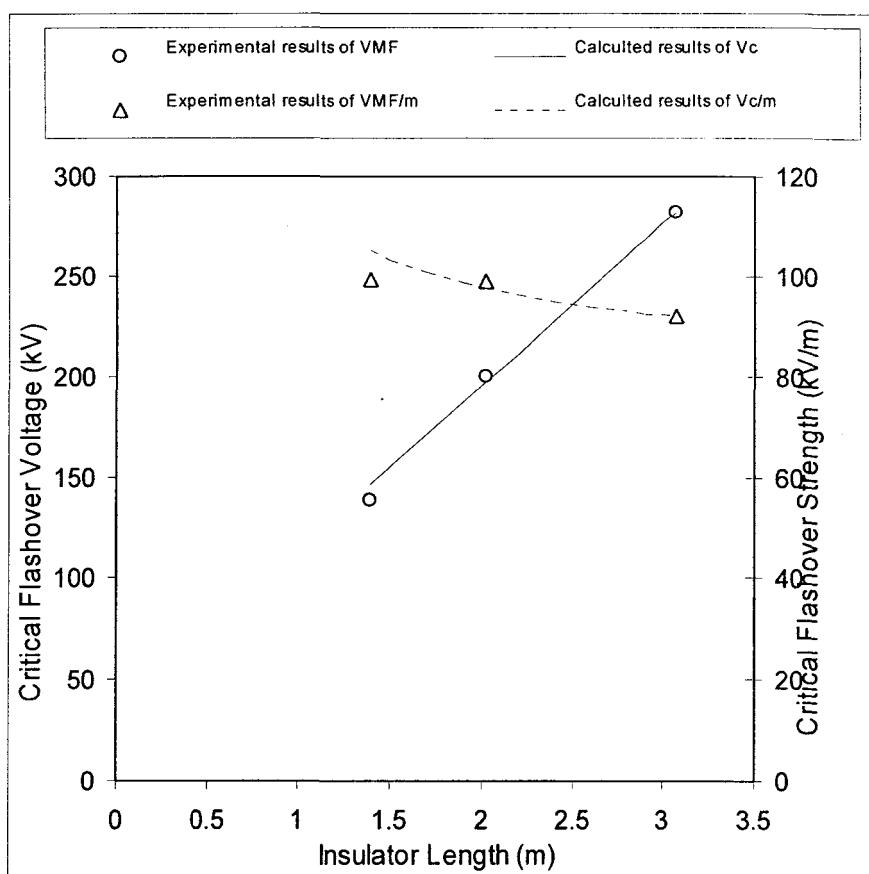


**Fig.5.8 Experimental results and those calculated from the improved model ( $\sigma = 30 \mu \text{ S/cm}$ )**

## 5.4 Application of the model

As an application, the improved model was used to calculate the critical flashover voltage ( $V_C$ ) of ice-covered insulators with different parameters, in order to study the effects of these parameters on  $V_C$ .

### 5.4.1 Effect of insulator diameter on $V_C$

The  $V_C$  was calculated as a function of insulator diameter, for a 15 mm ice thickness, 2.02 m dry arcing distance, and 80  $\mu\text{S}/\text{cm}$  applied water conductivity. As shown in Fig. 5.9, the minimum flashover voltage decreases as insulator diameter increases. However, the rate of decrease of flashover voltage decreases with the increase in the diameter.

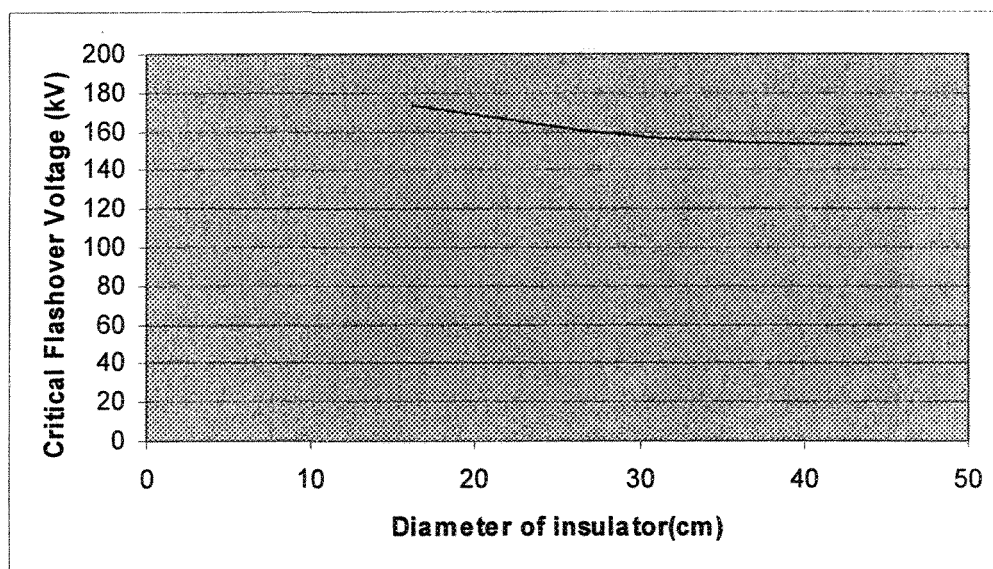


**Fig.5.9**  $V_C$  as a function of insulator diameter

### 5.4.2 Effect of conductivity on $V_C$

The effect of applied water conductivity was investigated using the improved model. For the parameters of 15 mm ice thickness, 26.2 cm insulator diameter, and 2.02 m dry arcing distance, the  $V_{MF}$  was calculated and is shown in Fig. 5.10. It can be observed that  $V_{MF}$  decreases with an increase in the freezing water conductivity.

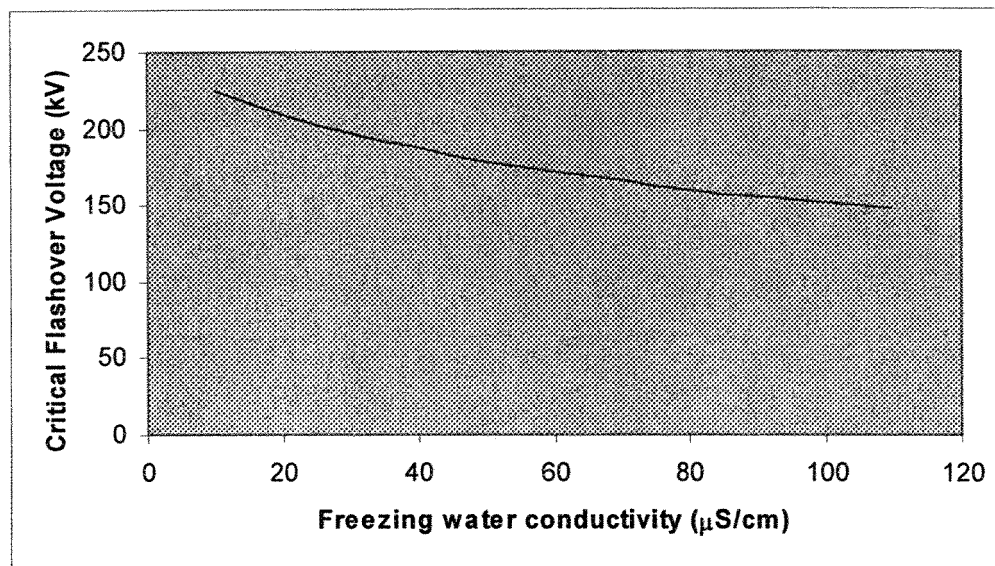


**Fig.5.10** Effect of freezing water conductivity on  $V_C$

### 5.4.3 Critical arc length and critical leakage current

From Equation 2.15, the critical reignition condition is:

$$V_m = \frac{kx}{I_m^b} \quad (5.7)$$

or

$$I_m = \left( \frac{kx}{V_m} \right)^{\frac{1}{b}} \quad (5.8)$$

Substituting  $I_m$  in Equation (5.5) with Equation (5.8), the following can be obtained:

$$V_m = Ax \left( \frac{kx}{V_m} \right)^{-\frac{n}{b}} + R(x) \left( \frac{kx}{V_m} \right)^{\frac{1}{b}} \quad (5.9)$$

Equation (5.9) presents a relationship between the peak value of applied voltage,  $V_m$ , and the length of arc,  $x$ . When the constants  $A$ ,  $n$ ,  $k$ , and  $b$  are determined,  $V_m$  will be uniquely determined by  $x$ . As  $x$  increases from 0 to the length of insulator ( $L$ ), the  $V_m$  will appear a maximum value ( $V_c$ ) at a critical value of arc length ( $x_c$ ) (See Fig. 5.6). Correspondingly, the leakage current is the critical current  $I_c$ . When the arc length,  $x$ , is less than  $x_c$ , the arc is stable, and longer arc lengths require higher applied voltages. When  $x$  is longer than  $x_c$ , longer arc lengths require lower voltages, which means that the arc is unstable and will extend rapidly until flashover. In the case of uniformly polluted insulators, and neglecting the current concentration at arc root, the percentage of the critical arc length is  $\frac{1}{n+1}$ , which is independent from the insulator length  $L$  [52].

In this case, the current concentration at arc root was considered and the critical arc length was calculated, as shown in Fig. 5.11. It may be observed that the percentage of critical arc length depends on the dry arcing distance of the insulator; it decreases with an increase in dry arc length for both conductivities of 30 and 80  $\mu\text{S}/\text{cm}$ .

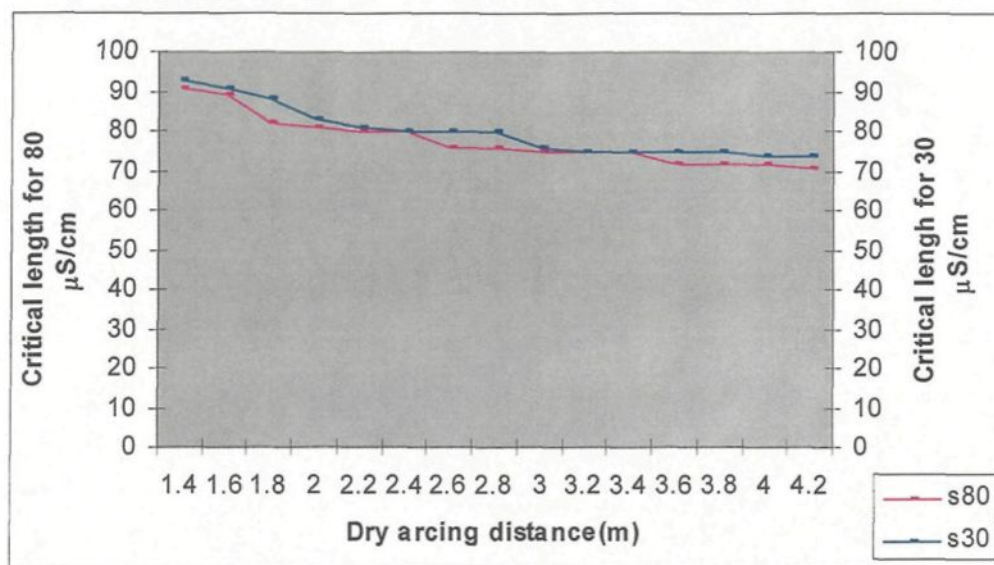


**Fig.5.11 Critical arc length as a function of dry arcing distance**

The corresponding leakage current at the critical arc length was also calculated. The results are listed in Table 5.5. It can be noted that the critical current is almost independent from the dry arcing distance; it increases only with an increase in applied water conductivity. These results are in agreement with those obtained by Hampton in the case of polluted insulators [34].

**Table5.5 Critical current calculated from the improved model**

Arcing Distance (m)	I <sub>c</sub> (A)	
	$\sigma = 30 \mu\text{S/cm}$	$\sigma = 80 \mu\text{S/cm}$
1.4	0.89	1.3
1.6	0.93	1.35
1.8	0.88	1.26
2	0.9	1.3
2.2	0.91	1.34
2.4	0.93	1.38
2.6	0.96	1.31
2.8	0.98	1.33
3	0.93	1.35
3.2	0.94	1.38
3.4	0.95	1.41
3.6	0.96	1.34
3.8	0.98	1.36
4	0.98	1.39
4.2	1	1.4

Finally, the improved model is helpful for understanding the mechanism of flashover phenomenon on long lengths ice-covered insulators, and a powerful tool for the design of outdoor insulators for cold climate regions.

## **CHAPTER 6**

# **CONCLUSIONS AND RECOMMENDATIONS**

## Chapter 6

# Conclusions and Recommendations

### 6.1 Conclusions

Using a standard post type insulator, a series of flashover tests were carried out to examine the flashover performance of EHV insulators covered with ice. An improved mathematical model was proposed for predicting the critical flashover voltage of ice-covered insulators. On the basis of the experimental results and their analysis the following conclusions may be drawn:

- 1). The atmospheric ice accreted on an insulator surface will markedly decrease their insulating strength. Due to the partial discharge activity during ice accumulation, there are usually two air gaps were formed along the EHV insulators, in series with the ice layer. Under applied voltage, two arcs were established along these two air gaps. Under certain condition, these two arcs propagated on the ice surface, and finally met, resulting in complete flashover.

- 2). The difference between the results obtained in “melting regime” and “icing regime” methods is less than 3 %. Therefore,  $V_{WS}$  for these two procedures can be considered to be the same, and both the melting and icing regime methods can be used for evaluating the flashover performance of ice-covered insulators in laboratories. For the melting regime, the maximum withstand voltage ( $V_{WS}$ ) is 195 kV<sub>rms</sub> for an applied water conductivity of 30  $\mu$ S/cm and an ice thickness of 15 mm, measured on a rotating monitoring cylinder. In comparison to the service voltage of the insulator ( $\sim 210$  kV<sub>rms</sub>), the maximum withstand voltage of the insulators under the test conditions is 7 % lower than the service voltage, which suggests that flashover may occur at service voltage under the test conditions.
  
- 3).  $V_{WS}$  increases with an increase in insulator dry arcing distance. The withstand stress slightly decreases as the dry arcing distance increases, which suggests that the maximum withstand voltage increases slightly non-linearly with the increase in insulator dry arcing distance.
  
- 4). Based on the experimental results, an improved mathematical model for predicting the minimum flashover voltage of ice-covered EHV insulators was proposed, using a two-arc model and adjusted the value of arc reignite constant  $k$  to 1,300. There is good concordance between the flashover voltage calculated from the improved mathematical model and those obtained from experiments. As an application, this model was used to study the effects of some parameters on the minimum flashover

voltage of ice-covered insulators: i) the minimum flashover voltage decreases with an increase in insulator diameter. However, the rate of decrease of flashover voltage decreases with the increase in diameter. ii)  $V_{MF}$  decreases with an increase in applied water conductivity.

- 5). The percentage of critical arc length depends on the dry arcing distance of the insulator. It decreases with an increase in dry arc length for both applied water conductivities of 30 and 80  $\mu\text{S}/\text{cm}$ . The corresponding critical current is almost independent from dry arcing distance; it increases only with the increase in the applied water conductivity.
- 6). The improved model is helpful for better understanding the flashover phenomenon on ice-covered insulators, and a powerful tool for the design of outdoor insulators in cold climate regions. More studies are needed to extend the present model to more general applications, for example, to predict the flashover performance of pre-contaminated insulators under ice and/or snow condition.

## 6.2 Recommendations

In this Master's study, a mathematical model for predicting the critical flashover voltage of long ice-covered insulators was established. However, due to time limitations, the mathematical model was validated only for STD porcelain post type insulators. In order to apply this model to engineering use, further studies are needed.

- 1). Since this model is validated only by the experimental results from STD porcelain post type insulators, more tests are needed for other types of insulators, for example suspension insulators, to validate the model, and to study the effects of insulator parameter on the model.
- 2). Because glaze is considered as the most dangerous type of ice to power systems, this model was established for predicting the critical flashover voltage of insulators completely covered with this type of ice. However, in order to advance our knowledge, snow and other types of ice, such as soft and hard rime, and particularly ice on pre-contaminated surfaces, should also be studied. Then, the model can be improved again and extended to these situations.
- 3). Light ice layers, which do not bridge insulator sheds, as well as insulators with booster sheds, should be studied further. In both cases, several air gaps can appear on the ice surface and, therefore, the multi-arc model should be considered.

## References

- [1] Bui, H. T., Phan, L. C., Huraux, C. and Pissolato, J., “HVDC Flashover on the Surface of Conductive Ice”, IEEE International symposium on Electrical Insulation, Montreal, Canada, Paper 84CH1964-6, pp. 85-88, 1984.
- [2] Chaarani, R., “Étude de l'Influence des Caractéristiques des Isolateurs sur Leurs Performances Électriques dans des Conditions de Givrage”, Ph.D. thesis, University of Quebec at Chicoutimi, 2003.
- [3] Chaarani, R., “Détermination de la tension de tenue maximale des isolateurs composites en EPDM.M.Sc.Thesis, UQAC,Fall 1996,121p.
- [4] Cherney, E. A., “Flashover Performance of Artificially Contaminated and Iced Long-rod Transmission Line Insulators”, IEEE Transactions on Power Apparatus and Systems, Vol. PAS-99, No. 1, pp. 46-52, February 1980.
- [5] Chisholm W.A., Tam, Y.T., ERVEN, C.C. and Melo ,T.O., (1993), “500 KV Insulator Performance under Contamination Ice, Fog, and Rising Temperature-Operating Experience and Field Studies”, IEEE Power Engineering Summer Meeting, 1-8.
- [6] Claverie, P. and Porcheron, Y., “How to Choose Insulators for Polluted Areas”, IEEE Transactions on Power Apparatus and Systems, Vol. PAS-92, No. 3, pp. 1121-1131, 1973.
- [7] Claverie, P., “Predetermination of the Behavior of Polluted Insulators, IEEE Transactions on Power Apparatus and Systems, Vol. PAS-90, pp. 1902-1908, 1971.

- [8] Drapeau, J.F., Farzaneh, M. and Roy, M.J., “An Exploratory Study of Various Solutions for Improving Ice Flashover Performance of Station Post Insulators”, Proc.of 10<sup>th</sup> International Workshop on Atmospheric Icing of Structures IWAIS’2002, Brno, Czech Republic, June.2002.
- [9] Erler,F. ,“Zum Kriechuberschlag Dicker Isolator en bei Wechsels Pannung”,Elektric,Vol.3 pp.100-102,1969.
- [10] Farzaneh, M. et al. 2003, Insulator Icing Test Methods and Procedure. A position paper prepared by the IEEE Task Force on Insulator Icing Test Methods. IEEE Transactions on Power Delivery, Vol. 18, No. 4, pp. 1503-1515, 2003.
- [11] Farzaneh, M. and Brettschneider, S., “Étude de la tension de tenue des isolateurs de postes en présence de glace atmosphérique en vue d’un choix approprié de type et configuration d’isolateurs de postes a 735 kV”Volume 1 : Étude en vue du choix d’isolateurs pour le future poste Monteregie.Presented to IREQ.Industrial Chair NSERC/Hydro-Quebec/UQAC on Atmospheric icing of power network (CIGELE),September 2001.
- [12] Farzaneh, M., Drapeau, J.F., Zhang, J., Roy, M. and Farzaneh, J., “Flashover Performance of Transmission Class Insulators under Icing Conditions, Proc. of the World Conference Exhibition on Insulators”, Arresters, Bushings (INMR), Marbella, Spain, pp. 306-316. 2003.
- [13] Farzaneh, M. and Kiernicki, J., “Flashover Performance of IEEE Standard Insulators under Ice Conditions”, IEEE Transactions on Power Delivery, Vol. 12, No. 4, pp. 1602-1613, October 1997.

- [14] Farzaneh, M. and Kiernicki, J., "Flashover Problems Caused by Ice Build-up on Insulators", IEEE Transactions on Electrical Insulation, Vol. 11, No. 2, pp. 5-17, March/April 1995.
- [15] Farzaneh, M., Kiernicki, J., Chaarani, R., Drapeaum, J. F. and Martin, R., "Influence of Wet-grown Ice on the AC Flashover Performance of Ice Covered Insulators", Proceedings of 9<sup>th</sup> International Symposium on High Voltage Engineering, Austria, Paper 3176, pp.1-4, 1995.
- [16] Farzaneh, M. Li, Y. Zhang, J. Shu, L. Jiang, X. Sima, W. and Sun, C. "Electrical Performance of Ice-Covered Insulators at High Altitudes", accepted by IEEE Transactions on Dielectrics and Electrical Insulation, 2004.
- [17] Farzaneh, M. and Melo, O.T., "Properties and Effect of Freezing and Winter Fog on Outline Insulators". Journal of Cold Regions Science and Technology, no.19 February 1990, pp.33-46.
- [18] Farzaneh, M. and Zhang, J., "Behavior of DC Arc Discharge on Ice Surfaces", Proceedings of 8<sup>th</sup> International Workshop on the Atmospheric Icing of Structures, Iceland, pp. 193-197, 1998.
- [19] Farzaneh, M. and Zhang, J., "Modeling of DC Arc Discharge on Ice Surfaces", IEE Proceedings Generation, Transmission and Distribution, Vol. 147, No. 2, pp. 81-86, 2000.
- [20] Farzaneh, M., "Effect of Ice Thickness and Voltage Polarity on the Flashover Voltage on Ice Covered High Voltage Insulators", Proceedings of 7<sup>th</sup> International Symposium on High Voltage Engineering, Dresden, Germany, Vol. 4, Paper 43.10, pp.203-206, 1991.

- [21] Farzaneh, M., "Ice Accretions on High-Voltage Conductors and Insulators and related phenomena", *Philosophical Transactions of the Royal Society*, Vol. 358, No. 1776, pp. 297-3005, November 2000.
- [22] Farzaneh, M., Zhang, J. and Chen, X., " DC characteristics of Local Arc on Ice Surface", *Atmospheric Research*, Vol. 46, pp.49-56, 1998.
- [23] Farzaneh, M., Zhang, J. and Chen, X., " Modeling of the AC Arc Discharge on Ice Surfaces", *IEEE Transactions on Power Delivery*, Vol. 12, No. 1, pp.325-338, 1997.
- [24] Farzaneh, M., Zhang, J. and Chen, X., "DC characteristics of Local Arc on Ice Surface", *Atmospheric Research*, Vol. 46, pp.49-56, 1998.
- [25] Fikke, S. M., "Possible Effects of Contaminated Ice on Insulator Strength", *Proceeding of the 5<sup>th</sup> International Workshop on the Atmospheric Icing of Structures*, Tokyo, Japan, Paper B4-2-(1), 1990.
- [26] Fikke, S. M., Hanssen, J. E. and Rolfseng, L., "Long Range Transported Pollution and Conductivity on Atmospheric Ice on Insulators", *IEEE Transactions on Power Delivery*, Vol. 8, No. 3, pp. 13411-1321, July 1993.
- [27] Fofana, I., Tavakoli, C. and Farzaneh M., "Modeling Arc Propagation Velocity on Ice-Covered Surfaces", *Proceedings of 10<sup>th</sup> International Workshop on Atmospheric Icing of Structures*, Brno, Czech Republic, pp. 1-6, 2002 June.
- [28] Fofana, I., "Dielectric Properties of Air and High Voltage", *Notes de cours 6DIG967*, UQAC, winter 2003.
- [29] Forest, J. S., "The Performance of High Voltage Insulators in Polluted Atmospheres", *Proceedings of IEEE Winter Meeting*, New York, 1969.

- [30] Fujimura, T., Naito K., Hasegawa Y. and Kawaguchi T.K. (1979), "Performance of Insulators Covered with Snow or Ice", IEEE Transactions on Power App. & Syst. Vol.PAS-98, pp. 1621-1631.
- [31] Gorski, R.A, (1986), "Meteorological Summary Multiple Outage on the Southern Ontario (Central Region) on 500 KV System", Ontario-Hydro, Met. Report, No.80604-1, 1-40.
- [32] Godard, S., "Mesure des gouttelettes de nuage avec un film de Collargol".Bulletin de l'observatoire du Puy de Dome, no.2, 1960, pp.41-46.
- [33] Guan, Z. and Huang, C., "Discharge Performance of Different Models at Low Pressure Air", Proceedings of 4th International Conference on Properties and Applications of Dielectric Materials, Brisbane Australia, Paper 5102, pp. 463-466, July 1994.
- [34] Hampton, B. F., "Flashover Mechanism of Polluted Insulation", Proceedings of IEE, Vol. 11, No. 5, pp. 985-990, 1964.
- [35] Hara, M. and Phan, C. L., "Leakage Current and Flashover Performance of Iced Insulators", IEEE Transactions on Power Apparatus and Systems, Vol. PAS-98, No. 3, pp. 849-859, 1979.
- [36] Hurley J.J. and Limbourn G.J. , "Correlation of Service Performance of Insulators and Lightning Arresters under Pollution Conditions with Test Results with a View to Examining the Validity of Present Criteria for Insulator Selection and Testing", CIGRE, SC. 33, September 1969.
- [37] Hydro-Quebec, "Ice-storm Damage Impacts on Current and Future R&D Activities at Hydro-Quebec", Electricity today, vol. 10, No. 5, pp 5-7, 1998.

- [38] Hydro-Quebec, "Analysis of the Hydro-Quebec System Blackout on April 1988", Official Hydro-Quebec Report, Montreal, July 1988.
- [39] IEEE Publication, IEEE Std 4, "IEEE Standard Techniques for High-Voltage Testing", p.129, October 1995.
- [40] Imai, I. and Chiro ,I., "Studies on Ice Accretion", Researches on Snow and Ice, No. 1, pp.35-44, 1953.
- [41] International Electrotechnical Commission (IEC), "Artificial Pollution Tests on High-voltage Insulators to be Used on A.C. Systems", International Standard 60507, 1991.
- [42] Kannus, K. and Verkkonen, V., "Effect of Coating on the Dielectric Strength on High Voltage Insulators", Proceeding of the 4<sup>th</sup> International Workshop on the Atmospheric Icing of Structures, Paris, France, pp.296-300, 1988.
- [43] Kawai, M., " AC Flashover Tests at Project UHV on ice-covered Insulators", IEEE Transactions on Power Apparatus & Systems, Vol. PAS-89, No. 8, pp. 1800-1805, Dec. 1970.
- [44] Khalifa, M. M. and Morris, R. M., "Performance of Line Insulators under Rime Ice", IEEE Transactions on Power Application and Systems, Vol. PAS-86, pp. 692-698, 1967.
- [45] Kuroiwa, D., "Icing and Snow Accretion", Monograph Series of Research, Institute of Applied Electricity, Japan, pp. 1-30, 1958.
- [46] Matsuda, H., Komuro, H. and Takasu, K., "Withstand Voltage Characteristics of Insulator String Covered with Snow and Ice", IEEE Transactions on Power Delivery, Vol. 6, No. 3, pp. 1243-1250, July 1991.

- [47] Neumärker, G., “Verschmutzungszustand und Kriechweg”, Monatsber. D. Deut. Akad. Wiss., Berlin, Vol. 1, pp. 352-359, 1959.
- [48] Obenaus, F., “Fremdschichtüberschlag und Kriechweglänge”, Deutsche Elektrotechnik, Vol. 4, pp. 135-136, 1958.
- [49] Oguchi, H. et al., “Icing on Electric Wires”, Researches on Snow and Ice, No. 1, pp.45-49, 1953.
- [50] Phan, C. L. and Matsuo, H., “Minimum Flashover Voltage of Iced Insulators”, IEEE Transactions on Electrical Insulation, EI-18-6, pp. 605-618, 1983.
- [51] Phan, C. L., Pirotte, P. and Trinh, N. G., “A Study of Corona Discharges at Water Drops over the Freezing Temperature Range”, IEEE Transactions on Power Apparatus and Systems, Vol. PAS-93, No. 2, pp. 724-734, 1974.
- [52] Rizk, Farouk A. M., “Mathematical Models for Pollution Flashover”, Electra, Vol. 78, pp. 71-103, 1981.
- [53] Schneider, H. M., “Artificial Ice Tests on Transmission Line Insulators-A Progress Report”, IEEE/PES Summer Meeting, San Francisco, USA, Paper A75-491-1, pp. 347-353, 1975.
- [54] Shu, L., Gu, L. and Sun, C., “A Study of Minimum Flashover Voltage of Iced-covered suspension Insulators”, Proceedings of 7<sup>th</sup> International Workshop on the Atmospheric Icing of Structures, Chicoutimi, Canada, pp. 87-92, 1996.
- [55] Su, F. and Hu, S., “ Icing on Overhead Transmission Lines in Cold Mountainous District of southwest China and Its Protection”, Proc. of 4<sup>th</sup> International Workshop on Atmospheric Icing of Structures, Paris, France, pp. 354-357, 1988.

- [56] Su, F. and Jia, Y., "Icing on Insulator String of HV Transmission Lines and Its Harmfulness", Proceeding of the 3<sup>th</sup> International Offshore and Polar Engineering Conference, Singapore, pp.655-658, 1993.
- [57] Vuckovic, Z. and Zdravkovic, Z., "Effect of Polluted Snow and Ice Accretion on High-voltage Transmission Line Insulators", Proceeding of the 5<sup>th</sup> International Workshop on the Atmospheric Icing of Structures, Tokyo, Japan, Paper B4-3, 1990.
- [58] Wilkins, R. and Al-Baghdadi, A. A. J., " Arc Propagation along an Electrolyte surface", Proceedings of IEE, Vol. 118, No. 12, pp. 1886-1892, 1971.
- [59] Wilkins, R., "Flashover Voltage of High Voltage Insulators with Uniform Surface Pollution Films", Proceedings of IEE, Vol. 116, No. 3, pp. 457-465, 1969.
- [60] Wu, D., Halsan, K. A. and Fikke, S.M., "Artificial Ice Tests for Long Insulator Strings" Proceedings of 7th International Workshop on the Atmospheric Icing of Structures, Chicoutimi, Canada, pp. 67-71, 1996.
- [61] Zhang, J. and Farzaneh, M., "Propagation of AC and DC Arcs on Ice Surfaces", IEEE Transactions on Dielectrics and Electrical Insulation, Vol. 7, No. 2, pp. 269-276, 2000.